This is to certify that the

dissertation entitled

KINETICS STUDIES OF ISOLATED REACTION STEPS IN BERTHELOT AMMONIA DETERMINATIONS

presented by

Robert George Harfmann

has been accepted towards fulfillment
of the requirements for

Ph.D. degree in Chemistry

Stanley R. Crouch
Major professor

Date 1/22/90

KINETICS STUDIES OF ISOLATED REACTION STEPS IN BERTHELOT AMMONIA DETERMINATIONS

By

Robert George Harfmann

A DISSERTATION

Submitted to
Michigan State University
in partial fulfillment of the requirements
for the degree of

DOCTOR OF PHILOSOPHY

Department of Chemistry

1990

ABSTRACT

KINETICS STUDIES OF ISOLATED REACTION STEPS IN BERTHELOT AMMONIA DETERMINATIONS

By

Robert George Harfmann

This dissertation involves studies of the Berthelot reaction for the determination of ammonia. Each of the three steps of the Berthelot reaction sequence have been isolated and studied. Substantial evidence is presented to verify that the reaction order for ammonia is one. Rate constants for the initial and final steps of the reaction sequence have been determined. The rate limiting step of the overall reaction has been found to be the reaction between monochloramine and phenol. The pentacyanoferrate compounds used to accelerate the reaction rate have been found to act directly on this rate-limiting step. These compounds have no effect on the initial reaction step and limited effect on the final reaction step.

The first evidence for the formation of benzoquinonechlorimine has been presented. This compound has long been postulated as an intermediate formed in the reaction between monochloramine and phenol. Benzoquinonechlorimine has been shown to react with pentacyanoferrate compounds to form a green product. This product has been observed in previous works, but the cause has not previously been identified.

The rate constant for the interfering reaction involving bromide ion has been determined. It has been found that the interference can

not be avoided by simple changes in reagent concentration or solution pH during ammonia determinations in saline solutions.

Stopped-flow mixing was employed for the collection of rapid kinetics data. Modifications made to the instrument to facilitate the studies presented in this dissertation have been described.

Dedicated to my Parents

Who taught me many of the important values in life;
who struggled so I could succeed;
who helped make this all possible.

ACKNOWLEDGEMENTS

Thanks first and foremost to Stan for providing the opportunity to work within a diverse research group and for his guidance during this research project. His discussions and comments in various settings often suggested new directions.

Thanks to the many Crouch group members for the help through the years: Keith, Pat, Gene, Paul, Mark and John, whose computer and electronics expertise helped prevent certain pieces of equipment from accidentally falling off the Chemistry Building roof. Thanks also to Marguerite and Kim for their special role in making the group more like a family. Thanks and good luck to the newer group members Steve, Larry, Chris and Mayda.

To the Linden Street gang: Arnie, Brian, Bruce, Frank, John, and Ren, thanks, the time went by too quickly. Now, ask me to identify that vegetable in 5 seconds or less.

Kim, Paul, and Pete, I will always remember the laughter, the fun, and the friendship.

TABLE OF CONTENTS

LIST OF TABLES

TABLE OF FIGURES

CHAPTER I

INTRODUCTION

Ammonia is a simple but important chemical present throughout our environment. Used as a source of nitrogen in the production of fertilizer, ammonia is also a waste product generated in many manufacturing processes. Ammonia can be found in biological fluids, where its presence can indicate the onset of certain diseases and its detection can allow for early treatment. Ammonia can also have a severe impact on the ecology, particularly in a marine environment where it readily forms compounds of a toxic nature. Consequently, for both health and environmental reasons, determinations of ammonia at trace levels have been important for several decades.

Clinical and environmental laboratories worldwide determine ammonia in a wide variety of sample matrices. Numerous analytical methods are available, each method having advantages which may be unique for the particular analytical requirements. Colorimetric detection is the most popular technique, but electrochemical and fluorometric detection methods are also common. Known methods for the determination of ammonia are being improved, and new procedures continue to be developed. The most widely employed analytical technique for the determination of ammonia involves its reaction with phenol and hypochlorous acid. This reaction is known as the Berthelot reaction. It is specific for ammonia, and sensitive spectrophotometric detection is possible due to the formation of an intensely blue colored

charge-transfer complex. Detection limits as low as 10^{-7} M NH_3 have been reported [1] for methods based upon this reaction. However, poor precision is often reported for such low level determinations.

The Berthelot reaction has many advantages which contribute to its popularity. In addition to being sensitive and specific, the instrumentation is inexpensive and easy to use. The reagents are prepared from inexpensive, stable compounds which are readily available. The entire reaction procedure is easily automated, and high sample throughput is possible. Much effort has been directed towards improving the precision of Berthelot reaction techniques and these have been largely successful. However, there are also limitations to the reaction such as severe interferences from the bromide ions present in saline solutions. Furthermore, the details of the reaction mechanism, particularly the nature and role of the catalyst, are not well understood.

The present research was undertaken to overcome some of the aforementioned limitations and to study the reaction and its interferences on a fundamental level. In this chapter, the history of the Berthelot reaction is presented to provide a framework to the research work presented in later chapters. A review of the use of pentacyanoferrate catalysts is also presented to indicate what is known about these compounds. Finally, the goals that characterize the present research are listed.

A. BERTHELOT REACTION HISTORY

In 1859, Berthelot [2] reported that an intense blue color developed as the result of a reaction between ammonia, hypochlorous acid and phenol. The reaction now bears his name, and it is the basis of the single most widely applied method for the determination of ammonia. However, the analytical potential of this reaction was slow to be realized. It was not until 1912 that Thomas [3] applied the reaction to the determination of ammonia in blood. After this, there were minor applications of the reaction. However, no significant research concerning the Berthelot reaction appeared in the literature until 1944. In that year, Russell [4] reported that Mn(II) ions catalyzed the reaction and gave a three-fold increase in sensitivity. She concluded that the end product of the reaction was indophenol or some related compound. Interest in the reaction grew and other catalysts, such as acetone [5], were soon reported. In 1954, Lubochinsky and Zalta [6] reported that sodium nitropentacyanoferrate significantly accelerated the rate of the Berthelot reaction. Discovery of this catalyst was of paramount importance. It was found that nitropentacyanoferrate increased the reaction sensitivity for ammonia to such a degree that sample preconcentration was no longer necessary. This compound, commonly known as nitroprusside, greatly simplified methods employing the Berthelot reaction. A host of analytical procedures based on nitroprusside catalysis of the Berthelot reaction have since appeared.

A mechanism for the reaction was first proposed by Bolleter and co-workers [7] in 1961, over one century after it was first reported by Berthelot. The mechanism proposed by these workers consisted of three

sequential reactions. Ammonia first reacts with hypochlorite ion to produce monochloramine. The monochloramine then reacts with phenol to form a quinone compound. In the presence of additional phenol, this quinone forms an indophenol. In basic solution, loss of a proton produces indophenolate ion which results in the intense blue color observed. Their reported reaction sequence is as follows:

$$OCl^- + NH_3 \longrightarrow NH_2Cl + OH^-$$

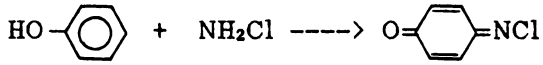

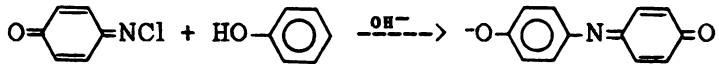

Although this reaction sequence is widely accepted as correct, Bolleter and coworkers did not attempt to verify their mechanism. The only evidence they report in support of the sequence is that phenol reacts with p-aminophenol under basic conditions to produce a blue compound with a spectrum identical to that of indophenol. Many studies have since been conducted on the Berthelot reaction; however, no concerted effort to study the isolated steps of the reaction has been made.

B. RESEARCH CONCERNING THE CATALYST

The discovery of an effective catalyst has, more than any other factor, been responsible for the widespread use of the Berthelot reaction. Although the reaction has many useful characteristics, it can be prohibitively slow without a catalyst. Several hours may be required for color development with NH_3 concentrations below the millimolar level.

Hence, the reaction only became important analytically after nitropentacyanoferrate was shown to be so effective. The literature concerning the Berthelot reaction from the mid-50's to present understandably shows an interest in the nitropentacyanoferrate compound. After reviewing this literature, Horn and Squire [8] developed a Berthelot reaction procedure using nitroprusside and acetone as catalysts. Their method offered improved sensitivity and accuracy over other methods available at that time. They later learned that the nitro group of the pentacyanoferrate compound is converted to a nitrito group in the presence of hydroxide ions. By using nitritopentacyanoferrate and omitting acetone entirely, sensitivity for ammonia was greatly improved [9]. This indicated that the nitrito complex was the true catalytic species. Mark [10] verified their results and suggested that the compound catalyzed the first step of the Berthelot reaction sequence. He did not, however, verify his suggestion.

The aqueous chemistry of pentacyanoferrate compounds has been widely studied. These compounds are known to undergo a wide variety of substitution processes [11-13]. It has been shown [14,15] that nitritopentacyanoferrate, in aqueous solution, is in equilibrium with a small amount of aquopentacyanoferrate. Patton [16], and Patton and Crouch [17] conducted studies to determine if aquopentacyanoferrate was the true catalyst. They found that the aquo complex did accelerate the production of indophenol. Furthermore, the compound was most effective when used in a 1:1 ratio with monochloramine. All previous procedures required a huge molar excess of the nitro and nitrito complexes. Such a large excess is inconsistent with the idea of a catalyst. Patton pointed out that a large excess of the nitro complex

would be necessary to produce an effective amount of the aquo complex in reacting solutions. This aquo complex could then catalyze the production of indophenol. Based on their studies, these workers developed a new procedure which further improved the sensitivity and precision of the Berthelot reaction.

A suprising result of the study by Patton and Crouch [17] was the fact that the aquo species was no longer present at the end of the reaction. Apparently the complex is destroyed during the reaction and is thus not a true catalyst. This fact has largely been ignored and so the fate of the complex is unknown.

C. GOALS OF THE RESEARCH

Although the reaction has been popular for so long, it has not been completely characterized. Numerous papers have reported the use of the Berthelot reaction for the determination of ammonia, as evidenced by a recent review [18]. These provide procedures which have been optimized for an analysis in a particular sample matrix. Unfortunately, it is often the case that conditions have been juggled to produce reasonable results without a careful examination of the kinetics of the reactions in progress. The result is that there has been much disagreement as to the optimum reaction conditions for the analysis of ammonia. At one time, it was even believed that two distinct reactions occurred depending on the order of the reagent addition [19,20].

This research was undertaken to accomplish several goals. The first goal was to isolate each step of the Berthelot reaction and to study the associated kinetics. Several successive reactions actually occur to

produce indophenol. Each of these steps is influenced to various degrees by the reaction conditions which exist in the sample solution. To treat the overall reaction as one step which is to be "optimized" is an incomplete solution. Given the flexibility possible with certain analytical techniques, such as continuous flow analysis, it is possible to manipulate individual steps and so optimize conditions, within limits, for that particular step. To do so requires a fundamental understanding of each individual step in the reaction sequence.

A second goal of the study was to determine the effect of the pentacyanoferrate complex on each of the isolated steps. It should not be suprising that the role of this compound is presently unknown when one realizes that the reaction sequence which it influences is also unknown. By determining its effect on each of the isolated steps, a better understanding of the role of this compound can be developed.

Another goal was to collect kinetics data for some of the interfering reactions involving bromide ions. An understanding of the kinetics of these interfering reactions leads to better control of reaction conditions to eliminate these interferences.

Once all of these steps are accomplished, it should be possible to use the information collected during these studies to develop a new procedure offering improved sensitivity, decreased reaction time, and the ability to analyze saline solutions without interferences from bromide ions.

CHAPTER II

STOPPED-FLOW INSTRUMENTATION

This chapter provides an introduction to the general theory and design of stopped-flow instruments. The home-built stopped-flow instrument used during a majority of the reaction-rate studies herein presented is described. The tests conducted to evaluate the system performance are presented. Finally, modifications made to the instrument over the course of these studies are described.

A. GENERAL CONSIDERATIONS

Several of the reactions under investigation occur at such a rapid rate that they reach completion seconds after the reagents are mixed. These reactions are too fast to be studied by methods using manual mixing. To obtain useful concentration measurements from such rapidly reacting systems, a method of mixing which is fast in comparison to the rate of reaction must be employed. The stopped-flow mixing technique is ideal for reaction-rate studies of certain rapid reactions. Its combination of speed and efficiency for both mixing and detection allows data to be collected on the millisecond time scale.

The stopped-flow method was first used by Chance in 1940 [21]. As in other flow methods, reagents are mixed in a flowing stream and pass on to some detector. The stopped-flow method differs from other flow methods in that the flowing stream is physically stopped. Data

collection begins only after the flow has ceased. A physical property of the solution is then monitored as the reaction progresses. In this way, the entire course of the reaction can be obtained from a single volume element. In theory, the reagents are instantaneously mixed and stopped in the observation cell. In practice, several milliseconds are required to mix the reagents, move them to the detector and stop the flow. The time required to complete this process is known as the instrument dead time. During this time mixing is incomplete and fresh solution continues to flow through the observation cell. Rate data collected during this time are not meaningful since no single volume element is monitored. A major part of the dead time is due to mixing. Mixing must be rapid and efficient if rapid reactions are to be followed. Efficient mixing requires that turbulent flow be induced in the reaction stream, which requires that high flow rates be achieved. Mixing chamber design is also critical in producing turbulent flow. Another advantage of high flow rates is that the reagent stream passes to the detector in a minimum amount of time. Once there, the flowing stream must be rapidly stopped before data collection can begin.

Detection in stopped-flow instruments can be accomplished by a variety of methods. Spectrophotometric detection is most common, but any property of the solution that is related to the concentration of either a reactant or a product can be used. This physical property is measured continuously (or nearly so) during the course of the reaction. The data obtained provide a reaction profile of the change in concentration with time. Mathematical treatment of these data yields the desired kinetics information.

There are many other important features of the stopped-flow technique. These range from further design considerations to the many detection schemes employed. These have been discussed in detail by Crouch, et. al. [22]. The next section presents the specific design of the instrument used during these studies.

B. THE STOPPED-FLOW INSTRUMENT

The stopped-flow instrument used to perform the reaction rate studies is shown in Figure 2.1. This instrument was originally built and described by P. M. Beckwith [23,24]. It has been modified by P. K. Notz [25], F. J. Holler [26], R. S. Gall [27], R. Balciunas [28], and R. B. Putt [29]. As illustrated, the instrument is modular in design, each section machined from stainless steel blocks. The stainless steel is inert to most chemicals and provides good thermal properties. Because temperature has such a great effect on the reaction rates, it must be carefully controlled during rate measurements. In addition to room temperature fluctuations, heat can be generated by dilution, viscous friction, and by the reaction being studied. The stainless steel blocks are channeled such that water can circulate throughout the system to allow for thermostatting. A Model E52 thermostatting unit (Haake Co., Saddlebrook, NJ) controls the temperature to within ±0.2 C.

Two valves in the instrument control the flow of the reagents. These valves consist of stainless steel rods which rotate in Teflon sleeves. Teflon is also chemically inert, but its low thermal conductivity makes thermostatting difficult. Because steel to steel contact in the valves is unsuitable, Teflon was used; the amount was kept to a

Stopped Flow Instrumentation

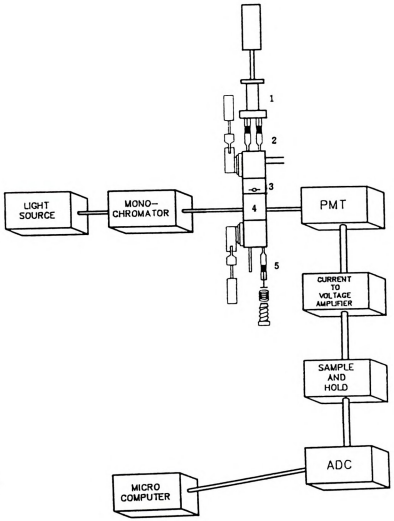

Figure 2.1 Stopped-flow instrument, including: (1) pressure-driven drive syringes, (2) reagent reservoirs, (3) mixing chamber, (4) observation cell, and (5) waste syringe.

minimum. Unfortunately, Teflon is subject to cold flow. Wear on these parts causes leaking which requires that the Teflon be replaced.

Plungers in the reagent reservoirs and the waste reservoir are also of stainless steel. Each plunger was fitted with double neoprene washers to ensure a tight seal with no sample carry-over. The reagent plungers are pneumatically driven at a pressure of about 65 psi. The valves which direct the flow of the reagents are also rotated by pneumatically driven cylinders. The waste plunger is spring-loaded to expel the solution after measurements are complete. The flow system is vertical to minimize problems caused by air bubbles in the observation cell. The entire system is controlled by a computer/instrument interface designed by E. H. Ratzlaff [30]. This controller is connected to an Intel 8085A based microcomputer designed by B. Newcome [31] and built by E. H. Ratzlaff. An opto-interrupter positioned at the waste valve detects when flow in the instrument has stopped and signals the microcomputer to begin collecting data. Software written by R. B. Putt [29] allows the user to select parameters for the collection of data.

Spectrophotometric detection is presently used in this system, although conductance has been used in previous studies [25]. The heart of the detection system is a Model EU-701-50 light source and a Model EU-700 monochromator (GCA McPherson Instrument Co.) coupled with a Model 1P28A photomultiplier tube (RCA Corporation). The PMT is connected to a model EU-42A photomultiplier power supply (Heath Co.). The light source is connected to the observation cell of the instrument by a quartz fiber optic bundle (Schott Optical Co.). A Keithley model 427 current amplifier (Keithley Instruments, Inc.) is used to perform the current-to-voltage conversion. The voltage is digitized by the

microcomputer ADC and stored for later analysis. The range of this ADC is 0-10 volts. Maximum precision in the collected data is obtained by using this entire range. A 10 V maximum output from the current amplifier is selected in several ways. One way is to change the monochromator slit width to vary the radiant intensity incident on the sample. This changes the output of the PMT. Another way is to increase the voltage supplied to the PMT, which will increase its gain. A third method is to increase the gain on the Keithley to increase the voltage output to the ADC. In practice, drawing more than 1 μA of current from the PMT can cause 'fatigue'. This results in slowed response which can destroy the rapid collection of data necessary during stopped-flow experiments. Since a 10 V maximum is desired from the current amplifier, this necessitates that the gain be set to no less than 10^7 V/A. The slit width is then usually set to 2000 um to provide maximum light throughput. It is the voltage supplied to the PMT that is adjusted to select a 10 V maximum corresponding to 100% transmittance. The operating range of the 1P28A is 400-1250 volts. By adjusting the high voltage power supply within this range, the 10 V maximum is easily set without changing the other parameters.

Once the reagents have been prepared, the instrument is controlled at a dedicated terminal. The user is prompted for reaction parameters, initiates the collection of data, and observes the experimental results in the form of a reaction progress curve displayed on a Tektronics oscilliscope. Reaction parameters can be changed and multiple runs can be conducted and averaged. Data that appear satisfactory can then be labeled and transmitted serially to a DEC LSI

PDP 11/23 minicomputer (Digital Equipment Corp.) for mass data storage and data manipulation.

C. PERFORMANCE OF THE INSTRUMENT

Before conducting reaction-rate studies of interest to this research, it was necessary to evaluate the performance of the stopped-flow instrument. The classical reaction between Fe^{3+} and SCN^- is ideal for such a test since the reaction is rapid and the kinetics are well understood [32-34]. In the reaction the two ions rapidly form a highly colored product that is easily detected spectrophotometrically. The instrument is used to collect transmittance data from this reaction. The data are then converted into rate information. Once the rate constant is determined, it is compared to the known rate constant value. One other advantage of these tests is that the data can be used to determine the dead time of the instrument through a graphical extrapolation [35]. Performing such tests periodically allows the user to be confident that measurements made during subsequent studies are not distorted by deadtime effects or leaks in the system. Because various parts of the instrument have been replaced, the system performance has been tested several times during these studies. The results obtained agree well with each other and with those obtained by previous users of this instrument. Typical results are provided below from one such system evaluation.

1. Experimental

Reagent grade chemicals were used to prepare solutions for these studies. All reactions took place at room temperature, which was maintained by means of thermostatting. The tungsten lamp was turned on and allowed to stabilize for 30 minutes before experiments were begun. The monochromator was adjusted to 450 nm, the wavelength of maximum absorbance for the iron-thiocyanate product. A slit width of 2000 μm was selected. The maximum voltage was set to 9.90 V. A rise time of 0.03 μs was selected for the Keithley current amplifier.

A stock solution of 0.0100 M Fe^{+3} was prepared by dissolving 0.2706 g $FeCl_3 \cdot 6H_2O$ (J. T. Baker Chemical Co.) in 100 mL distilled water. A 0.0400 M stock solution of SCN^- was then made by dissolving 1.9436 g of KSCN (Fisher Scientific Co.) in 100 mL distilled water. A series of standard iron solutions were then prepared from the stock solution by diluting various volumes of the stock solution in volumetric flasks. An Eppendorf model 4710 digital pipet (Brinkmann Instruments Inc., Westbury, NY) was used to prepare the solutions. The iron standards were diluted with 0.05 M H_2SO_4 (Mallinkrodt, Inc.) to provide acidic conditions and adjust the ionic strength. The range in concentration was between 3-10 x 10^{-4} M Fe^{3+}. The stock solution of KSCN was then diluted 1:10 to produce a 0.004 M working solution of SCN^- that was also 0.05 M in H_2SO_4.

2. Discussion

The reaction between Fe^{+3} and SCN^- is reversible. Under the constant pH conditions used in these studies, the reaction can be written as shown below:

$$Fe^{3+} + SCN^- \rightleftharpoons Fe(SCN)^{2+} \qquad (2.1)$$

The following rate equation applies:

$$d[Fe(SCN)^{2+}]/dt = k_1[Fe^{3+}][[SCN^-] - k_{-1}[Fe(SCN)^{2+}] \qquad (2.2)$$

Initial rates were used to analyze the data. Very little of the product has formed during this initial part of the reaction. The reverse reaction is thus negligible and can be ignored. Rate data were collected for the series of iron solutions reacting with the thiocyanate. The reaction curve is generated from one single volume element. Data are collected for either four or eight such volume elements during one 'experiment'. Individual results from each data set are averaged together to help improve precision. At least two such data sets were collected for each of the iron solutions in the series. For each data set, the initial portion of the reaction rate curve was selected and its slope was measured using a linear regression program. Results are listed in Table 2.1. This initial slope is equal to the initial reaction rate. By plotting the initial rate verses the initial concentration of iron, it is possible to determine the rate constant for the reaction. Such a plot yields a straight line with a slope of 5476 absorbance units per second. Dividing this value by the path length of the cell, the molar absorptivity of the product (4630 $\underline{M}^{-1}$ cm^{-1}), and by the concentration of thiocyanate gives a second order rate constant value of 316 $\underline{M}^{-1}$ s^{-1}. This value falls well within the literature values which range from

TABLE 2.1
Iron thiocyanate reaction calibration data

Solution	$[Fe^{+3}]x10^4$	slope
1	1.50	0.7078
		0.7282
2	2.50	1.170
		1.123
3	3.00	1.493
		1.585
4	3.50	1.697
		1.702
5	4.00	1.962
		1.985
6	4.50	2.334
		2.256
7	5.00	2.648
		2.643
		2.529
		2.648

Data for the reaction of Fe^{+3} with SCN^-. The slope is measured from the initial portion of the reaction curve.

200-400 $\underline{M}^{-1}$ s^{-1}. Similar values have resulted from all such evaluations performed after each modification made to the instrument. They indicate that the kinetics results obtained during these studies should be accurate and reliable.

In another test, the stock solution of iron was mixed together with the thiocyanate solution and data were collected for ten separate reactions. The initial reaction rate was determined for each data set and the precision of the stopped-flow instrument was evaluated. The test results are given in Table 2.2. The value of 1.79% RSD indicated that the instrument provides reproducible results for the rate studies conducted.

Finally, the instrument dead time was determined by extrapolating the rate curve until it intersects with the line for blank absorbance. This point marks the time when the reagents first come into contact and a product begins to form. The difference in time between this point of intersection and the first recorded data point is the dead time. A value of 6 ± 1 ms was determined for the instrument. This agrees well with previously determined values ranging from 5 ± 1 ms to 8 ± 1 ms on this instrument [23,24,28,29]. It also indicates that rapid reactions can be easily followed.

D. RECENT MODIFICATIONS

The stopped-flow instrument has been modified in several ways during the course of this research. These changes provide the user with increased flexibility in the collection of spectrophotometric data and

TABLE 2.2
Iron thiocyanate reaction precision study

Solution	slope x 10^3
1	2.758
2	2.731
3	2.667
4	2.806
5	2.755
6	2.788
7	2.811
8	2.671
9	2.710
10	2.833

Average slope = 2.753×10^{-3}
Std. deviation = 4.94×10^{-5}
RSD = 0.0179 = 2%

improved precision for slower reaction-rate information obtained in the UV region. These modification are described below.

1. Dual-beam Spectrophotometric Detection

Pseudo-order reaction-rate studies often require relatively low concentrations for one or more reagents. These conditions result in slower reaction rates which may require data collection to continue for tens of seconds. During such prolonged data collection times, the stopped-flow UV light source was observed to drift in intensity. The obvious result was error in the rate data. In the past, R. S. Gall [26,27] designed a double-beam system to correct for this problem. A pellicle beamsplitter was added to the instrument to split off a portion of the incident radiation. This portion was used as a reference to monitor the fluctuations in the source intensity. Kinetics data collected from the sample could then be corrected for these fluctuations.

The system Gall developed was effective in correcting for fluctuations in source intensity. However, the stopped-flow instrument has since undergone considerable change. A different computer and different software control the instrument. The instrument is no longer configured for dual-beam operation. In addition, a pellicle beamsplitter is not useful in the UV region. To allow data collected during these studies to be corrected for drift, both hardware and software changes to the instrument were required.

An inexpensive UV beamsplitter (ESCO Products, Inc., Oakridge, NJ) was purchased and added to the instrument. This beamsplitter directs about 30% of the incident radiation to a second RCA 1P28A

photomultiplier tube. Both PMTs are connected to the same EU-42A power supply. This ensures that any drift in the power supply will affect both PMT's equally and help keep the detection closely matched. The current to the reference PMT is amplified and converted to voltage by a home-built current-to-voltage converter constructed by D. Christman [36]. The voltage passes to the microcomputer and is collected and stored simultaneously with the sample data. The dual channel stopped-flow instrument is illustrated in Figure 2.2.

This new configuration presented a further problem in terms of memory space for the data storage. The total memory of the microcomputer was 32K, most of which was taken up by the downloaded software. The remaining memory was not sufficient to collect, store and process the reference channel data. It was thus necessary to add 8K of memory to the microcomputer. After this memory was installed, the software controlling the data acquisition was rewritten to access this extra memory and to process the reference channel along with the sample channel. Memory is allocated for the sample and reference values, each sufficient to contain up to four hundred data points. As each measurement is made, the separate digitized voltage values are stored in memory. After data collection is complete, a digital voltage value is recalled from memory and placed on a stack. The dark current value is then subtracted from this value. Next, the corresponding voltage from the reference channel is placed on the stack and corrected similarly for the dark current. The ratio of these two values is proportional to the ratio of the transmitted radiant intensity to the incident radiant intensity, or the sample transmittance. However, since the microcomputer performs integer arithmetic only, the fraction would

Stopped Flow Instrumentation

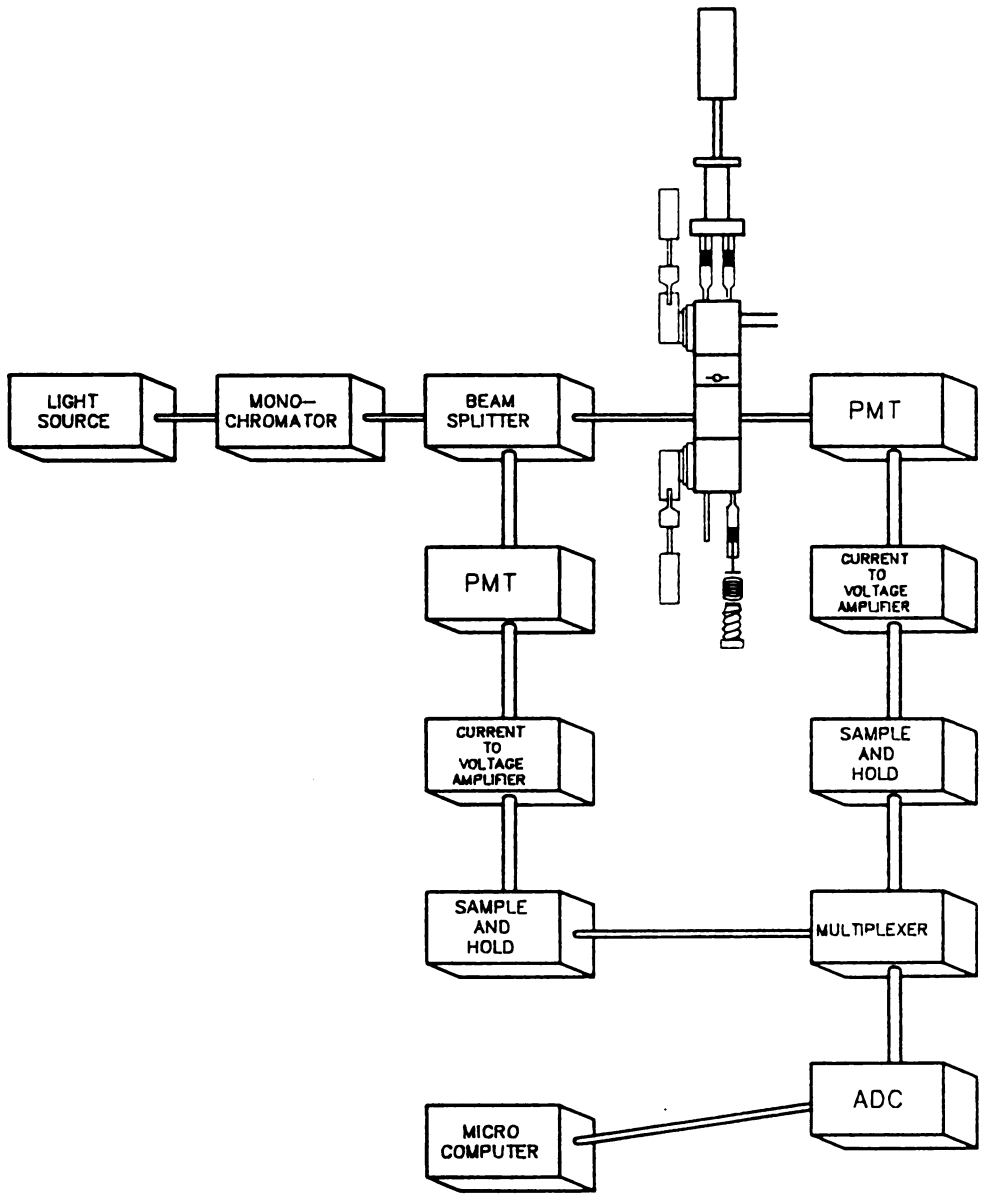

Figure 2.2 Stopped-flow instrument with a double-beam configuration.

be lost. It is necessary to multiply the fraction by a large constant to preserve significant figures. In calculating the transmittance, the corrected sample-channel voltage is converted to a double precision number and multiplied by 30,000. Then it is divided by the corrected reference value and stored. This entire process is then repeated for every data point collected. When the data are sent to the minicomputer for further processing, the factor of 30,000 is removed and the logarithm of the resulting fraction provides the absorbance.

After all of the hardware and software changes had been made, the ability of the set-up to correct for large fluctuations in the source intensity was tested. This was done by blocking off portions of the incident light, in increasing larger steps, while data collection was in progress. Water was used in the observation cell so that the only changes in intensity at the PMT's were due to the amount of light blocked. A stairstep signal was thus presented to each PMT, as seen in Figure 2.3. The corrected signal is shown in as a noisy but flat signal of intensity 1 in Figure 2.3. The instrument was thus shown to be capable of correcting for even drastic fluctuations in the source during the collection of data.

2. Diode array Detection.

Spectrophotometric detection of either a reactant or a product provides useful kinetics information in reaction rate studies. In many chemical systems, numerous species absorb during the course of the reaction. Any of these species can be followed spectrophotometrically to obtain useful rate data. Unfortunately, most instruments collect data

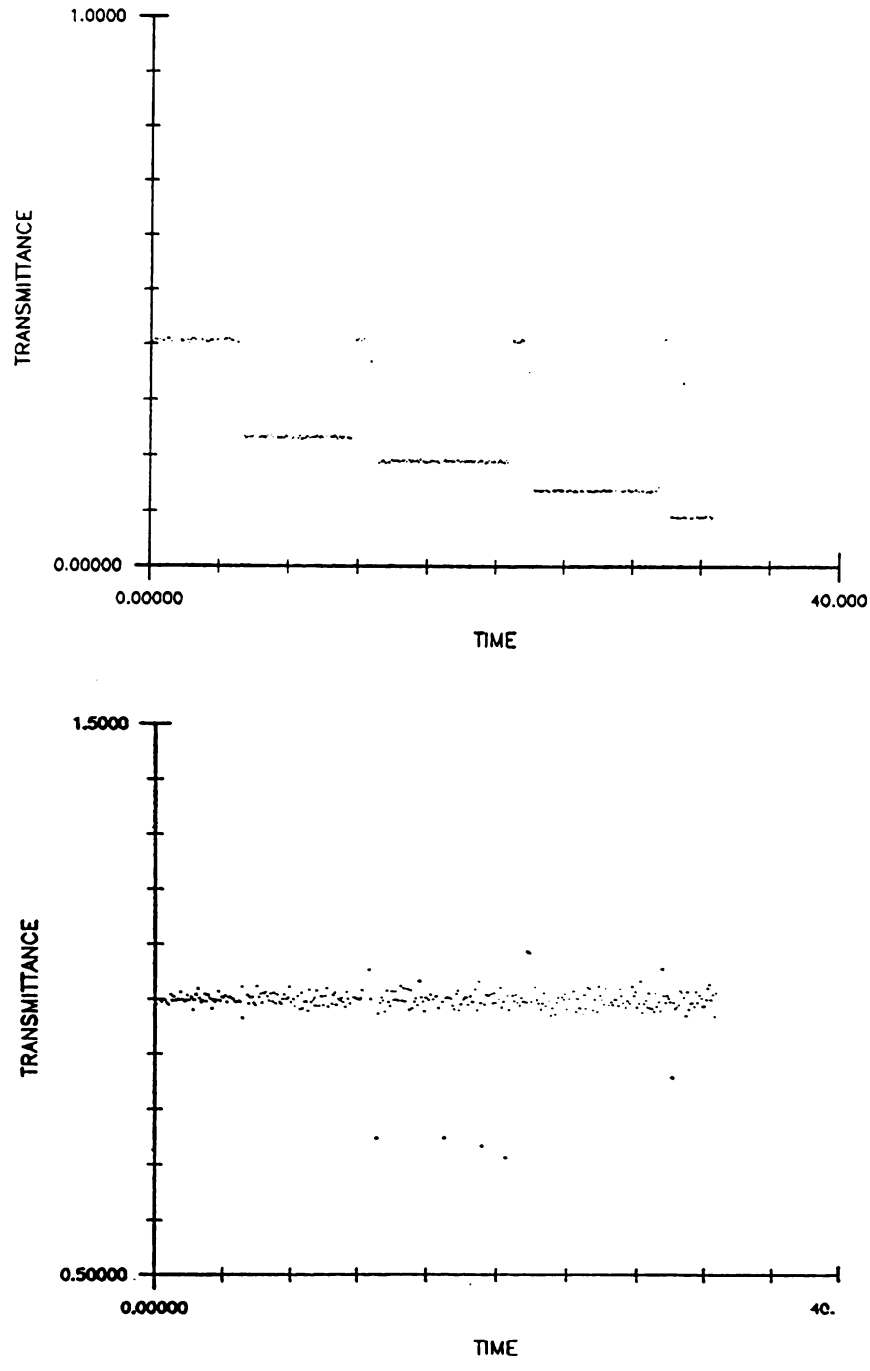

Figure 2.3 Simulated noise input into the detector (upper plot) and the detector output after correction with the double-beam reference signal (lower plot).

from one wavelength at a time. To collect data from several species requires multiple experimental runs. This requires the voltages to be reset after every wavelength change. Dye and Feldman [37] were the first to employ a rapid scanning detection system capable of obtaining reaction spectra over a wide wavelength range. Rapid scanning or diode array detectors make it possible to follow several absorbing species as a reaction goes to completion. This can add considerable power to the stopped-flow technique. Not only can the disappearance of a reactant be correlated with the appearance of a product, but intermediates may also become obvious, where as before they may have escaped detection.

A diode array detector was built and characterized by M. A. Victor [38]. It was then made available for the stopped-flow instrument. Connecting the two was a fairly easy task. The monochromator was not needed and so was removed. After removing the PMT, a quartz fiber optic bundle (Highlight Fiber Optics, Nampa, ID) was connected to the light pipe of the observation cell via a threaded sleeve built by the Chemistry Department Machine Shop. The other end of the fiber optic bundle connects to the diode-array. The opto-interrupter used to signal data collection to begin was also removed. A mechanical switch located in its place signals the end of the stopped-flow plunger stroke. All flow in the instrument stops and the switch is simultaneously triggered. The diode-array senses the signal and begins data collection under the preselected conditions. The instrument appears as shown in Figure 2.4. The array allows data to be collected over a 400 nm wavelength range. The 512 elements contained in the array provide a

Multidimensional Stopped Flow Instrumentation

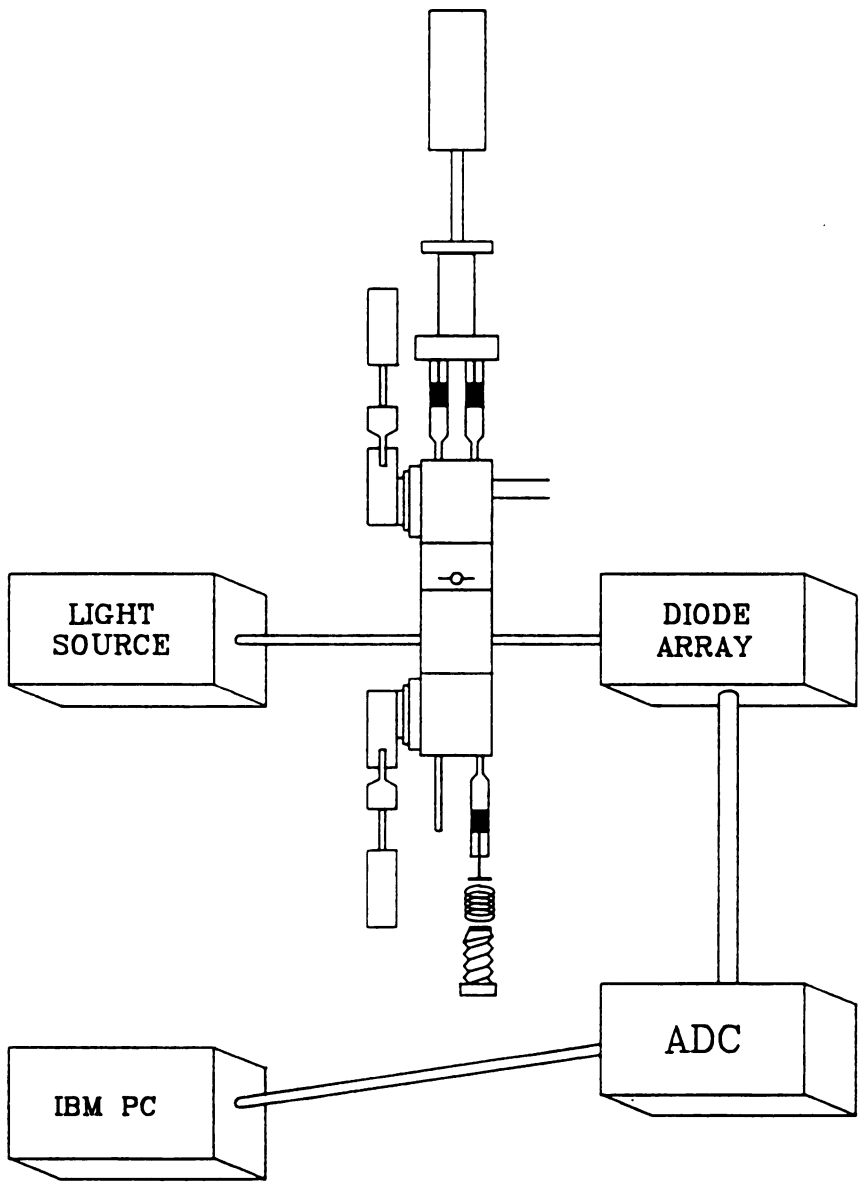

Figure 2.4 Stopped-flow instrument set up with the diode-array detector.

resolution of 0.7825 nm per element. At its fastest rate, a 400 nm scan can be completed every four milliseconds.

CHAPTER III

THE REACTION BETWEEN HYPOCHLOROUS ACID AND AMMONIA

This chapter concerns the first step of the Berthelot reaction. Pertinent literature regarding this reaction is reviewed. This literature consistently indicates that the maximum reaction rate is at a pH near 8 and that the ionic strength of the solution has little effect on the reaction rate. However, large discrepancies exist between these reviewed works, and questions concerning the reaction kinetics remain unanswered. Research undertaken to determine the reaction order for NH_3 and the rate constant is described. Finally, the effect of the coupling reagent on this reaction step is described.

A. HISTORICAL

According to the mechanism proposed by Bolleter and co-workers [7], the Berthelot reaction begins when OCl^- reacts with NH_3 to produce monochloramine. These workers did not study this initial Berthelot reaction step, but due to the toxic nature of the chloramines produced, other workers have [39]. Kinetics data for the production of monochloramine was first reported in 1949 by Weil and Morris [40]. Their attempt to study the reaction in detail was limited by the rate at which they could mix the reagents and collect data. They did learn that the reaction rate is very pH dependent. With a solution pH between 6.5 and 10.95 the reaction was complete within the time required for them to

mix the reagents. Outside of this range, the rate became slow enough to study. These workers collected spectrophotometric data at periodic intervals to follow the course of the reaction. They also determined the hypochlorite and total active chlorine concentrations by periodic titrations of reaction aliquots. The reaction data obtained from both methods agreed well. Rate data were collected under various conditions of pH, ionic strength, and temperature.

The strong pH dependence of the reaction is easily understood. Acid-base equilibria dictate that HOCl, OCl^-, NH_3, and NH_4^+ can all exist in the reaction mixture. Changing the pH between 6-11 significantly alters the equilibrium concentration of these species. The concentration of the reactive forms of the two reagents thus strongly depends on the pH of the solution during the reaction. The variation of the rate with pH can be explained equally well by a mechanism in which the reactive forms were both neutral or both charged. Because of the rapid equilibria involved, it is kinetically impossible to distinguish between these mechanisms. Weil and Morris found that ionic strength did not influence the reaction rate. Kinetics studies with similar amines led them to favor a mechanism between neutral molecules. They developed a second order reaction model which best fit their data with a reaction rate constant of 6.2×10^6 $\underline{M}^{-1}$ s^{-1}. Extrapolation of the model indicated a maximum reaction rate occurring slightly above pH 8.

With the development of rapid mixing and rapid data acquisition systems, it became possible to study the reaction in the pH range 8 to 11. Most Berthelot reaction procedures take place within this pH range since the benefits include shorter reaction times and greater colorimetric response. Patton and Crouch [16,17] used stopped-flow mixing to study

the reaction with respect to the Berthelot procedure. As in the work of Weil and Morris [40], Patton found that the maximum rate occurred near pH 8 and dropped off rapidly as the pH varied. Using distribution diagrams Patton observed that, relative to each other, the concentrations of HOCl and NH_3 are maximum slightly above pH 8. In a second order reaction, the reaction rate is directly proportional to the product of the concentrations of the two reagents. If the reaction is between the two neutral forms, the maximum rate should occur when the concentrations were maximum relative to each other. He thus concluded that the reaction was between the two neutral molecules. Patton reported a second order rate constant value of 4.8×10^4 $\underline{M}^{-1}$ s^{-1}.

The reaction appeared in the literature again in 1978 when Margerum, Gray, and Huffman [41] published studies of the formation of N-chloro compounds during the chlorination of water. They employed stopped-flow mixing to collect rate data for the reaction. Pseudo-first-order conditions were used, with NH_3 in excess. Data were obtained for the reaction in the pH range from 6 to 9.5. They reported a second order rate constant of 2.8×10^6 $\underline{M}^{-1}$ s^{-1} (0.1 $\underline{M}$ $NaClO_4$). These workers also studied the reaction of HOCl with a series of amines. They found that the rate constant increased as the base strength of the amines increased. This suggests that the mechanism is nucleophilic attack by the amine on the HOCl. Unfortunately, the evidence is not conclusive for NH_3 since it does not at all correlate with this trend in their study.

The most recent report in the literature concerning HOCl and NH_3 is due to Johnson and co-workers [42]. They used stopped-flow mixing and pseudo-first order conditions to study the reaction. Based on a series of experiments at high ionic strength (0.031 to 0.406 $\underline{M}$), they

obtained a rate constant of 3.1×10^6 M^{-1} s^{-1}. A later plot of the observed rate constant as a function of pH gave them a second order rate constant of 2.8×10^6 M^{-1} s^{-1} and a maximum rate near pH 8.2. They found that ionic strength has a slight effect on the reaction rate. When results from low ionic strength studies (0.003 to 0.006 M) were considered, they obtained a second order rate constant of 2.6×10^6 M^{-1} s^{-1}. These values agree well with the value reported by Margerum [41]. However, they are roughly half of the value initially reported by Weil and Morris [40]. Vastly different concentration of ammonia were used in the reaction rate studies. Johnson and co-workers [42] noted these large concentration differences and suggested that the reaction order for NH_3 might not be one. They tested this hypothesis and determined that the reaction order for NH_3 was 0.8.

The reaction has been studied under second order and pseudo-first order conditions. Results from these studies agree on the effect of pH and ionic strength. However, there is disagreement on the values of the rate constant and the reaction order for NH_3. Furthermore, there are problems with the reported results. Weil and Morris [40] could not study the reaction in the pH range important for the Berthelot procedure. Patton [16] failed to note from his distribution diagram that the concentrations of OCl^- and NH_4^+ are also maximum relative to each other at a pH slightly above 8. Thus, it cannot be concluded that the reactive forms are the neutral molecules. He also did not properly resolve the effect of pH from his reported rate constant. Johnson and co-workers [42] calculated rate constants based on a pseudo-first-order reaction model. However, examination of their experimental conditions shows an ammonia to hypochlorite concentration ratio of 15:1; this does

not sufficiently create pseudo-first-order conditions. Furthermore, their reaction order value of 0.8 was based on a plot of three experimental points; N_T was varied by a factor of 3 in the study. They performed no other studies to verify this somewhat surprising conclusion. If correct, the reaction mechanims need be reconsidered and the rate constant would need to be determined based on a model incorporating this reaction order value.

B. REACTION ORDER FOR AMMONIA

A necessary step of any kinetics study is to determine the effect of concentration on the reaction rate. Recent evidence suggests a reaction order of 0.8 for NH_3 in the $HOCl/NH_3$ reaction [42]. Such a non-integral reaction order indicates a more complex reaction mechanism than assumed in earlier studies. Until the true order is known, a rate constant for the reaction can not be determined. This section describes the experiments done to elucidate the reaction order for NH_3.

1. Reagent Preparation

The reagents described below were used to prepare solutions for the following reaction order studies as well as for the kinetics studies described in later sections of this chapter. All reagents were used without further purification, unless otherwise noted.

a. Hypochlorite solutions

Commercially available liquid bleach was used as a stock for all hypochlorite solutions. Such bleach solutions typically contain 5.25% by weight sodium hypochlorite. The total hypochlorite concentration in these bleach solutions was determined by iodometric titration. The concentration of this stock of hypochlorite was typically about 0.78 M. The bleach was kept refrigerated to minimize loss of the hypochlorite. Appropriate amounts of the bleach were diluted with distilled water to prepare the desired hypochlorite solutions.

b. Ammonia solutions

Ammonium chloride (J.T. Baker) was used as the source for NH_3 throughout these studies. The dried salt was dissolved in distilled water and was kept slightly acidic to minimize evaporative loss of NH_3. Appropriate volumes of the stock NH_4Cl solution were pipetted into volumetric flasks to prepare reagents of the desired concentrations. In all cases, data were collected from the reagents within an hour of preparation of the stock ammonia solution.

c. Buffers.

A stock solution of 0.050 M sodium borate (Fisher Scientific Company) was used to prepare buffers. Addition of 0.1 M HCl or 0.1 M NaOH to the sodium borate stock solution allowed buffers to be adjusted within the pH range of 8 to 11.

A potassium dihydrogen phosphate (Mallinckrodt) stock solution was used to prepare buffers in the pH range 7 to 8. Appropriate

amounts of 0.10 M NaOH were added to the stock solution to adjust the pH within this range.

2. Experimental

In order to determine the reaction order for ammonia, its concentration was isolated as a reaction variable. This is best accomplished under pseudo-first-order conditions. For each reaction order study, a series of solutions was prepared to establish pseudo-first-order conditions. Some experiments were done using hypochlorite as the limiting reagent while in others the ammonia was limiting. Solutions were buffered to maintain a constant pH in the reacting mixtures. An appropriate volume of 6 M sodium perchlorate was added to adjust each solution to an ionic strength of 0.1 M. Before mixing, the solutions were placed in a thermostatting water bath to equilibrate to constant temperature. Solutions were then mixed in the stopped-flow instrument described in chapter 2. Since NH_3 does not absorb in the UV and since the absorption band for HOCl is weak, the course of the reaction must be followed by observing either the disappearance of OCl^- at 292 nm or the appearance of NH_2Cl at 445 nm.

3. Results and Discussion.

The reaction between HOCl and NH_3 can be written as:

$$HOCl + NH_3 \longrightarrow NH_2Cl + H_2O \qquad (3.1)$$

Since the reaction order for NH_3 is uncertain, the reaction rate can be expressed in terms of the unknown order, n, and the reagent

concentrations as follows:

$$RATE = k_1[HOCl][NH_3]^n \quad (3.2)$$

HOCl and NH_3 establish separate equilibria in solution due to the exchange of protons with water.

$$HOCl + H_2O \rightleftharpoons OCl^- + H_3O^+ \quad (3.3)$$

$$NH_3 + H_2O \rightleftharpoons NH_4^+ + OH^- \quad (3.4)$$

Proton exchange occurs so rapidly that it does not influence the rate of reaction 3.1. However, as reaction 3.1 proceeds, the individual equilibria shift to form more of the two neutral molecules. It is thus the change in the total analytical concentration of each reactant that indicates the extent of the reaction. The total hypochlorite concentration, Cl_T, is given by:

$$Cl_T = [HOCl] + [OCl^-] \quad (3.5)$$

and the total ammonia concentration, N_T, is given by:

$$N_T = [NH_3] + [NH_4^+] \quad (3.6)$$

Using the equilibrium constant expressions for reactions 3.3 and 3.4, Equations 3.5 and 3.6 can be rewritten as:

$$[HOCl] = \frac{Cl_T}{(1 + K_a/(a_H \cdot \gamma))} \quad (3.7)$$

$$[NH_3] = \frac{N_T}{(1 + K_b \cdot a_H/(K_w \cdot \gamma))} \quad (3.8)$$

where Ka is the acid dissociation constant for HOCl; K_b is the base dissociation constant for NH_3; and γ is the activity coefficient for the ionic species. If the pH remains constant during the reaction, all values in the denominators of Equations 3.7 and 3.8 are constant. Substituting Equations 3.7 and 3.8 into Equation 3.2 and collecting constants gives:

$$RATE = k'[Cl_T][N_T]^n \quad (3.9)$$

Equation 3.9 indicates the dependence of the rate on the total analytical

concentration of both hypochlorite and ammonia. The observed rate constant of Equation 3.9 is given by:

$$k' = \frac{k_1}{(1 + K_a/(a_H \cdot \gamma))(1 + K_b \cdot a_H/(K_w \cdot \gamma))^n} \qquad (3.10)$$

a. Excess Ammonia

Under pseudo-first-order conditions with ammonia in excess, N_T remains essentially constant throughout the reaction. The concentration term can thus be collected into the observed rate constant and Equation 3.9, written in terms of the rate of change of total hypochlorite, gives:

$$(dCl_T/dt) = k''[Cl_T] \qquad (3.11)$$

Integration of Equation 3.11 leads to:

$$\ln[Cl_T] = k''t + \ln[Cl_T]_0 \qquad (3.12)$$

Where $[Cl_T]_0$ is the total hypochlorite concentration at the start of the reaction. It has been shown [43] that Equation 3.12 can be expressed in terms of any physical property of the solution that is linearly related to concentration. In terms of absorbance, A, Equation 3.12 becomes:

$$\ln(A - A_f) = k''t + \ln(A_0 - A_f) \qquad (3.13)$$

where A_f is the final absorbance at the completion of the reaction. The left side of Equation 3.13 can be calculated for every absorbance point collected. This value can be plotted versus the corresponding time to yield a line with a slope of k''. The rate constant of Equation 3.12 is

$$k'' = k'[N_T]^n \qquad (3.14)$$

Taking the logarithm of k'' gives:

$$\ln(k'') = \ln(k') + n \cdot \ln[N_T] \qquad (3.15)$$

For a series of solutions with varying N_T, a plot of $\ln(k'')$ versus $\ln[N_T]$

should result in a line with a slope equal to the reaction order for ammonia.

A series of solutions was prepared to provide pseudo-first-order reaction conditions with ammonia in excess. The solutions were all buffered to a pH of 10.45 and the ionic strength was adjusted to 0.01 M. The solutions were mixed in the stopped-flow instrument and the reaction was monitored by following the absorbance of OCl^- at 292 nm. A FORTRAN program was written based on Equation 3.13 and used to analyze the collected data. The program linearized the data and linear regression analysis of the line provided values of k'' for each solution. Table 3.1 lists the values obtained from these experiments. Values of k'' listed in Table 3.1 are the average values obtained from several independent runs. These values were used to obtain the reaction order according to Equation 3.15. Linear regression analysis of the log-log plot provides a slope of 0.91. Another such experiment with similar concentrations yielded a slope of 1.06. These values indicate that ammonia has a reaction order of 1 and not 0.8 as previously reported [42].

b. Excess Hypochlorite

Under pseudo-first-order conditions with hypochlorite in excess, Cl_T remains constant and Equation 3.9 can be written as:

$$\text{RATE} = k''[N_T]^n \qquad (3.16)$$

It can be shown that for any value of n, the initial rate is proportional to the initial concentration of ammonia to the n^{th} power. At the start of the reaction (for time=0):

$$(\text{RATE})_0 = k''\cdot([N_T]_0)^n \qquad (3.17)$$

TABLE 3.1
Determination of the reaction order for NH_3

Solution	$[N_T]$	Avg. k′	$\ln[N_T]$	$\ln(k')$
1	0.0518	36.947	-2.9604	3.6095
2	0.05365	37.635	-2.9253	3.6279
3	0.0555	38.942	-2.8914	3.6621
4	0.05735	40.655	-2.8586	3.7051
5	0.0592	41.374	-2.8268	3.7227

Values of k′ are determined from the slope of a plot of $\ln(\Delta A)$ vs. time. Columns 4 and 5 are the x,y pairs plotted to determine the reaction order. Linear regression analysis of the resulting line gives:

Slope = 0.91
Std. Error of Estimate = 8×10^{-3}
Variance of the Slope = 6×10^{-3}

Taking the logarithm of both sides of Equation 3.17 gives:

$$\ln(\text{RATE})_0 = n \cdot \ln[N_T]_0 + \ln(k'') \qquad (3.18)$$

A plot of the logarithm of the initial rate versus the logarithm of $[N_T]_0$ should yield a line with a slope equal to the reaction order for ammonia.

Preliminary experiments over a limited concentration range indicated that the reaction order is one. To determine the reaction order over a wider range of ammonia concentrations proved to be difficult. When $[N_T]_0$ is below 10^{-5} M, the change in absorbance during the reaction, ΔA, is too small to measure on the stopped-flow instrument. When $[N_T]_0$ is above 10^{-4} M, the hypochlorite concentration required to produce pseudo-first-order conditions is so high that the reaction becomes too rapid to follow. Even within these limits, the pH must be about 10.5 or above or the reaction half-life approaches the dead-time of the instrument. A series of ammonia solutions was prepared in the range 2×10^{-5} M N_T and 1.5×10^{-4} M N_T. Each solution was adjusted to an ionic strength of 0.10 M and buffered to a pH of 10.52. Each of these solutions was then mixed with 0.0065 M Cl_T adjusted to the same pH and ionic strength. Absorbance data were collected by monitoring ΔA for NH_2Cl at 445 nm. The collected data were strongly influenced by noise. This was particularly true for the least concentrated solutions, for which ΔA was no greater than 0.02 absorbance units. Up to 28 experimental runs were made for each solution. Subsequent point by point averaging of these runs helped to improve the S/N ratio for the collected data.

Even with averaging, noise in the data made measurement of initial rates very subjective. To decrease the influence of noise, the entire reaction curve was analyzed using a simplex curve-fitting routine

written by Wentzell [44]. Equation 3.16 was used to derive a mathematical model based on a reaction order of one. The integrated rate expression was written in terms of absorbance, time, an observed rate constant and other constants characteristic of the solutions. The model was written into the program and fit to the data by varying a set of adjustable parameters to minimize the sum of the square of the residuals. Three adjustable parameters were used in the reaction model: k'', A_0, and A_f. Although the latter two are fairly well known, they were made adjustable parameters since slight errors in these values can cause deviations in the fit. The program prints out the adjusted parameter values along with statistics of the fit. The final results can be plotted to visually check the fit. A good reaction model will necessarily reproduce the actual data for the entire range of concentrations tested. Since the adjustable parameters used in the model are often approximately known, these parameters can be compared with the 'known' values.

The program was run for each averaged data set until a consistent value of the sum of the square of the residuals was achieved. Figure 3.1 shows a typical fit of the model to the data. An excellent fit was obtained for each of the solutions tested. In every case the final values of A_0 and A_f agreed with the observed experimental values for those data.

From Equation 3.17 we see that the initial reaction rate equals the product $k''[N_T]_0$. The fitting routine returns a value for k'' for each fit. Since $[N_T]_0$ is known, the theoretical initial rate can be calculated for each solution. This calculated value is free from the inherent subjective bias of measuring an initial slope from data containing noise.

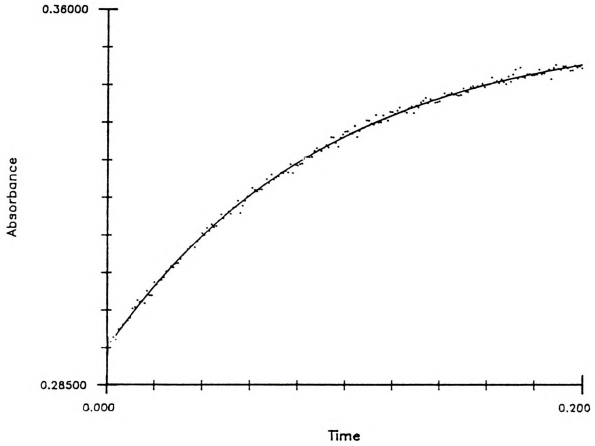

Figure 3.1 Fit of the reaction model to the experimental data. Reaction model is based on a reaction order of 1.0 for NH_3. Plotted points are actual data. Solid line is the fit of the model to the data.

Table 3.2 lists values of the initial slope and of the logarithms of the slope for each data set. A log-log plot of the data is shown in Figure 3.2. Linear-regression analysis of the resulting line provides a value of 1.02 for the slope; this slope equals the reaction order for NH_3.

A reaction model based on Equation 3.16 and a reaction order of 0.8 was then written into the simplex non-linear fitting routine. The program was used to analyze the same data to see how well this model could reproduce the data. A good fit was achieved with a reaction order of 0.8, as shown in Figure 3.3. However, Figure 3.4a shows the non-random deviations in the residuals of the fit for one of the solutions. These deviations followed a consistent pattern for each experimental run; although the visual fit is good, a reaction order of one statistically reproduces the data more precisely. The residuals of the fit for a 1.0 order reaction model are shown in Figure 3.4b.

Since Equation 3.16 is valid for this reaction model, the appropriate log-log plot should be linear with a slope equal to the reaction order. As before, values of k'' were obtained for each fit. These values were used to calculate the initial rates. The resulting log-log plot shown in Figure 3.5 does produce a line. Linear-regression analysis of the line provides a value of 1.02 for the reaction order for NH_3.

As a final test, the non-linear fitting routine was supplied with a model in which the reaction order was an adjustable parameter. When this model was fit to the data, it reproduced the data well at each concentration tested. Figure 3.6 shows a typical fit of the model to the data. Since the reaction order was a parameter, a 'best fit' value was returned by the program. The reaction order values in the range of

Table 3.2
Determination of the reaction order for NH_3

$[N_T]x10^5$	$k^{\sim a}$	$(Rate)_o$ [b]	$\ln[N_T]_o$	$\ln(Rate)_o$ [c]
1.989	10.9824	0.1789	-10.8254	-1.7212
2.983	10.6227	0.2595	-10.4200	-1.3492
4.971	11.2070	0.4562	-9.9091	-0.7849
5.966	11.1608	0.5452	-9.7268	-0.6066
7.955	10.8641	0.7076	-9.4391	-0.3458
9.943	11.3995	0.9281	-9.2160	-0.07465
11.93	11.2485	1.0988	-9.0336	0.0942
14.92	11.3646	1.3884	-8.8105	0.3281

[a] Values of $k^{\sim}$ determined by non-linear fit of the data.
[b] The theoretical value of $(Rate)_o$ is calculated from $k^{\sim}x[N_T]_o$.
[c] Columns 4 and 5 are the x,y pairs plotted to determine the reaction order. Non-linear regression analysis of the plot of $\ln(Rate)_o$ vs. $\ln[N_T]_o$ gives:

Slope = 1.02336
Standard error of estimate = 1.927×10^{-2}
Variance of the slope = 1.1×10^{-4}
Intercept = 9.34104

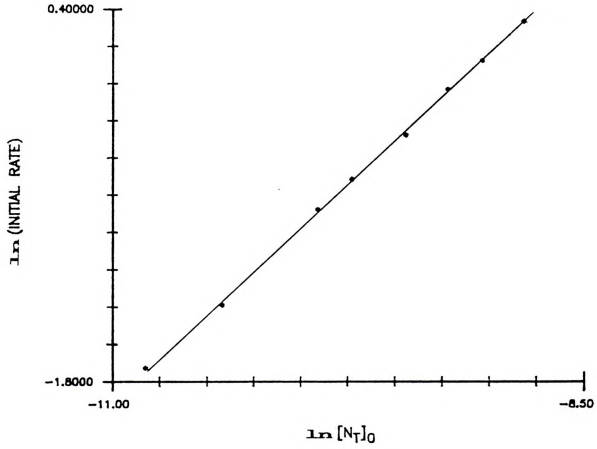

Figure 3.2 Plot to determine the reaction order for NH_3. Initial rates are determined from values of k_{obs} returned by the fitting routine. The slope of the line equals the reaction order.

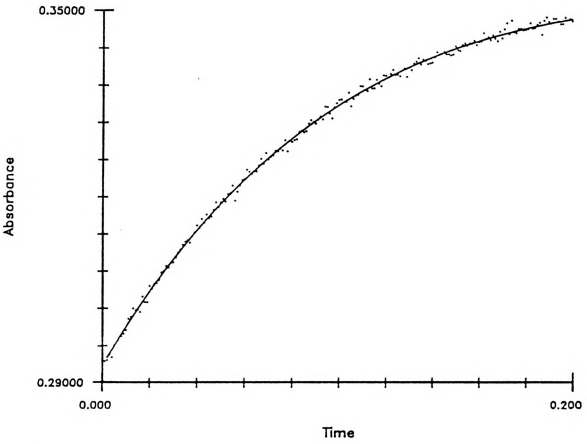

Figure 3.3 Fit of the reaction model to the experimental data. This reaction model is based on a reaction order of 0.8. Plotted points are actual data. Solid line is the fit of the model to the data.

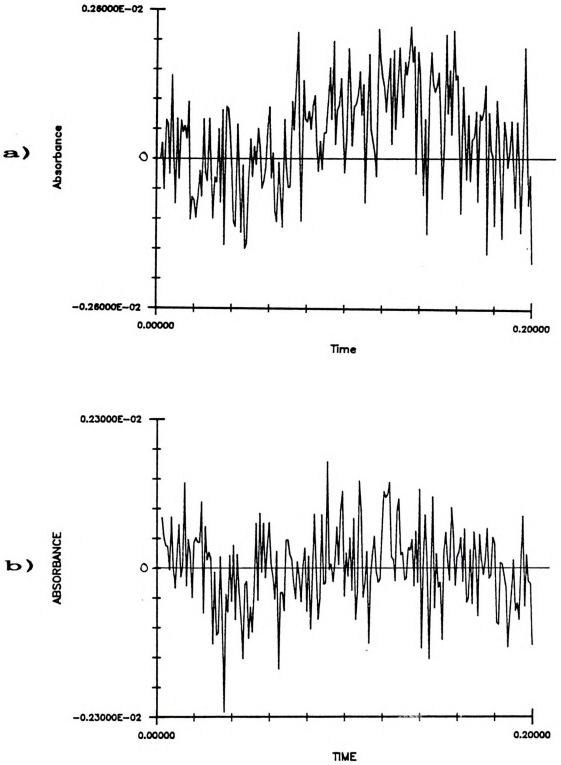

Figure 3.4 Residuals of the fitted data. a) Residuals for the 0.8 order reaction model. b) Residuals for the 0.8 order reaction model.

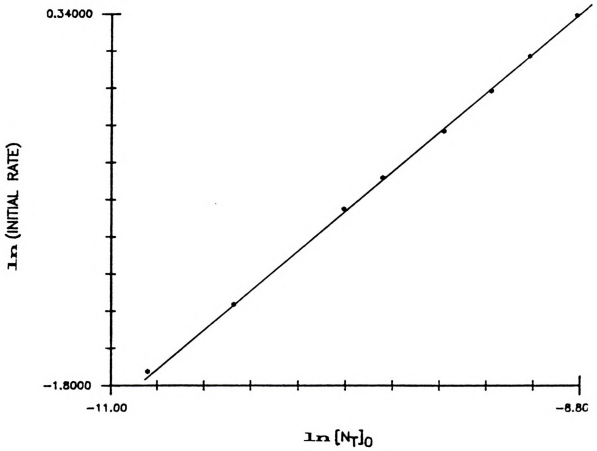

Figure 3.5 Plot to determine the reaction order for NH_3. Data analyzed using a 0.8 order reaction model.

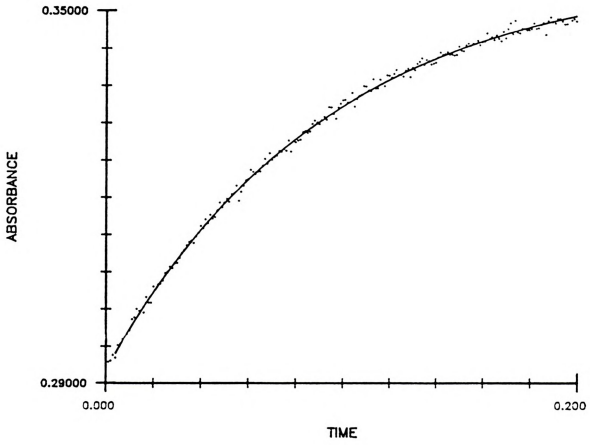

Figure 3.6 Fit of the variable order reaction model to the experimental data. Plotted points are actual data. Solid line is the fit of the model to the data.

0.93 to 1.03 were returned after each fit. The reaction order values for these experiments all indicate a reaction order of one for NH_3.

C. EVALUATION OF THE RATE CONSTANT

Equation 3.10 clearly indicates how the reaction rate constant depends on the reaction order for ammonia. Unless n is known, a value for k_1 can not be calculated from the experimentally determined rate constant. The above studies show that the reaction order for ammonia is one; the reaction between HOCl and NH_3 is thus a second order process. All equations derived in the last section are thus valid for values of n equal to one. It is now possible to determine k_1 based on these equations. This section describes the studies done to determine the second order rate constant.

1. Experimental

Pseudo-first-order conditions were used in the experiments to determine the reaction order for NH_3. Now that the reaction order is known, the same data can be analyzed to determine the second order rate constant.

The rate constant was also determined under second order conditions. Solutions were prepared such that the two reactants would be present in roughly equal concentrations. As before, all solutions were adjusted to a constant ionic strength with $NaClO_4$. Buffers were used to maintain a constant pH. Temperature was controlled by

thermostatting and reagents were used as quickly as possible to minimize evaporative losses.

2. Results and Discussion

a. Pseudo-first-order Conditions.

Rate constant values can be determined under various experimental conditions. The most common method is to study the reaction under pseudo-first-order conditions and measure initial rates. Equation 3.17 indicates how the initial reaction rate is proportional to the initial concentration of the limiting reagent. The initial rate is measured as the initial slope of the reaction curve. A plot of initial rates versus initial concentrations of the limiting reagent yields a line with a slope equal to k'. The value of k_1 is then determined through simple calculations. Although valid results can be obtained by the initial rate method, a significant portion of the data is ignored. Useful information about the reaction can be lost.

Another method to determine k_1 makes use of Equations 3.11-3.13, in which the rate equation is expressed in terms of the absorbance of the solution. The left side of Equation 3.13 is plotted versus time to obtain a line with a slope equal to k'. This method makes use of data from the entire reaction. However, it is sensitive to small errors in the value of A_f; any such errors can result in significant curvature in the resulting plot [43].

A third method involves non-linear fitting of a reaction model to the collected data. Equation 3.13 can be written such that the

absorbance is separated from other parameters. This results in:

$$A = (A_0 - A_f) \exp\{k''t\} + A_f \qquad (3.19)$$

The 'known' values on the right side of the equation can be used to calculate A_t. In non-linear fitting, values on the right side of Equation 3.19 are varied until the sum of the square of the residuals between the actual value of A_t and the calculated value have been minimized.

Non-linear fitting has already been used to analyze the pseudo-first-order data collected in the previous study. A wide concentration range was covered and the data is equally useful for the determination of k_1. Equation 3.19 was written into the earlier described program of Wentzell [44]. The results of the fit were used to produce the plot shown in Figure 3.2. The slope of the line gave the reaction order for NH_3. As indicated in Equation 3.13, the intercept of the line provides a value of k'' which represents the entire data. Linear-regression analysis of the line produces an intercept of 9.341; this value equals $\ln(k'')$. The observed rate constant is given by:

$$k'' = \frac{k_1 \varepsilon b \cdot [Cl_T]}{(1 + K_a/(a_H \cdot \gamma))(1 + K_b \cdot a_H/(K_w \cdot \gamma))} \qquad (3.20)$$

The activity coefficient, γ, is determined from the extended Debye-Huckel equation for an ionic strength of 0.10 M. The measured pH gives a value for a_H. K_a is 3.2×10^{-8}, from the value of Farkas, et. al. [45] and K_b is 1.774×10^{-5}, from the values of Bates and Pinching [46]. The molar absorptivity, ε, is 445 M^{-1} cm^{-1} (determined for the stopped-flow instrument during these studies) and the path length is 1.84 cm [27]. Since $[Cl_T]$ is known, k_1 is easily calculated. Assuming no errors in the above 'constants' (experimental errors only), the calculated result is $k_1 = (3.20 \pm 0.04) \times 10^6$ M^{-1} s^{-1}. The standard deviation of the rate

constant is calculated through use of the standard error of the estimate from the linear regression analysis. Although the 'constants' used do in fact have associated uncertainties, the only one of significance is the value of K_a for HOCl. If a more precise value for K_a is determined, a more meaningful value of k_1 can be derived.

b. Second Order Conditions.

The second order rate expression given in Equation 3.9 cannot be integrated directly. However, the change in concentration of the two reagents is linearly related. Equation 3.9 can be written in terms of an extent of reaction variable, x. This gives:

$$d[x]/dt = k'(a-x)(b-x) \tag{3.21}$$

where a and b represent the initial concentrations of the two reactants. Integration of Equation 3.21 leads to the familiar expression:

$$\frac{1}{b-a} \ln \frac{a\cdot(b-x)}{b\cdot(a-x)} = k't \tag{3.22}$$

For a reaction which goes to completion, where reagent a is present in limiting quantities, it has been shown [43] that

$$a/(a-x) = (A_f-A)/(A_f-A_0) \tag{3.23}$$

It likewise is shown for the non-limiting reagent, b, that

$$b/(b-x) = (A_f-A_0)/[(A_f-A_0) - (a/b)(A-A_0)] \tag{3.24}$$

Substitution of Equations 3.23 and 3.24 into Equation 3.22 yields, after rearranging:

$$\ln \frac{(A_f-A_0)-(a/b)(A-A_0)}{(A_f-A)} = k'(b-a)t \tag{3.25}$$

Since the equilibrium constants for HOCl and NH_3 are known, along with the initial reagent concentrations, and since the pH can be measured, all

that remains is to follow the absorbance during the course of the reaction. By applying Equation 3.25, the rate constant for the reaction can be determined.

A reaction model based on Equation 3.25 was written into the previously described simplex fitting routine [44]. The program was used to analyze data collected from experiments done under second-order conditions. The model reproduced the data very accurately, showing only random noise in a plot of the residuals. Figure 3.7 shows the fit to the data for disappearance of OCl^- at 292 nm. Rate constant values returned by the fitting routine were used to determine the second-order rate constant. Table 3.3 lists values of k' and the calculated values of k_1. The rate constant determined from this series of experiments is $(3.24 \pm 0.05) \times 10^6\ \underline{M}^{-1}\ s^{-1}$.

Another series of second-order experiments was done to determine the rate constant from data collected by monitoring the appearance of NH_2Cl at 245 nm. The model again closely fit the data as seen in Figure 3.8. Table 3.4 lists the values of k' returned by the fitting routine and the calculated values of k_1. The rate constant determined from this series of experiments was $(3.0 \pm 0.3) \times 10^6\ \underline{M}^{-1}\ s^{-1}$. The loss of precision in this set of results is due to the small ΔA obtained during the reaction. This lead to a smaller signal to noise ratio and a subsequent decrease in precision. Nevertheless, the rate constant agrees well with the values obtained from other studies under other reaction conditions.

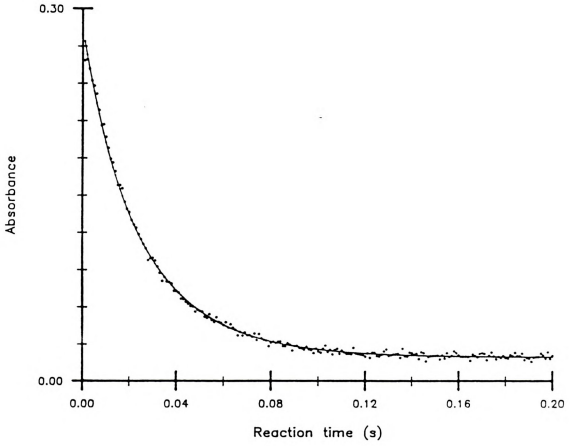

Figure 3.7 Fit of a second-order reaction model to the experimental data. Data was collected by following the disappearance of OCl^- at 292 nm.

TABLE 3.3
Determination of the second order rate constant

Solution	k'[a]	$k_1 \times 10^{-6}$
1	17,598	3.246
2	17,731	3.271
3	17,811	3.285
4	17,558	3.239
5	17,309	3.193
6	17,681	3.216
7	17,694	3.264
8	17,829	3.289
9	17,159	3.165
10	16,981	3.132
11	17,436	3.216
12	17,604	3.247
13	17,747	3.274

[a] Values of k' are from a non-linear fit of the pseudo-first-order data.

Avg value: $k_1 = 3.237 \times 10^6$
Std. deviation = 4.8×10^4

rate constant: $k_1 = (3.24 \pm 0.05) \times 10^6\ M^{-1}\ s^{-1}$.

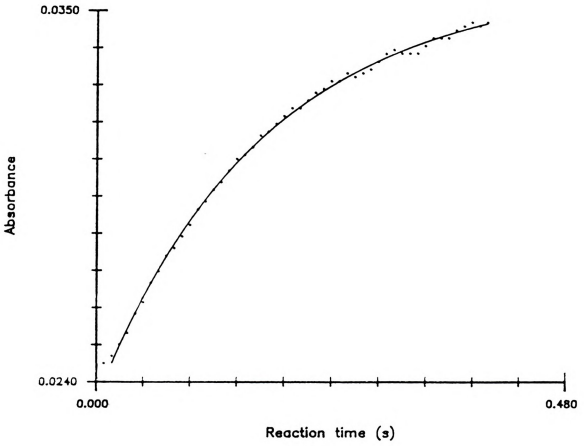

Figure 3.8 Fit of a second-order model to the data for the appearance of NH_2Cl at 245 nm.

Table 3.4
Determination of the second order rate constant

Soln.#	$[N_T] \times 10^5$	k'[a]	$k_1 \times 10^{-6}$
1	1.02	24,133	2.89
		23,067	2.76
		26,223	3.14
2	1.05	22,519	2.69
		24,569	2.94
3	1.08	22,283	2.67
		24,877	2.98
4	1.11	27,255	3.26
		25,506	3.05
5	1.14	27,142	3.25
		23,526	2.81
6	1.17	31,237	3.74
		26,301	3.15
		24,541	2.94
7	1.20	24,669	2.95
		24,410	2.92
		25,887	3.10

[a] Values of k' obtained from a non-linear fit of second order data.

average $k_1 = 3.012 \times 10^6$
standard deviation $= 2.56 \times 10^5$

rate constant : $k_1 = (3.0 \pm 0.3) \times 10^6\ M^{-1}\ s^{-1}$

D. EFFECT OF THE COUPLING REAGENT

This section describes the synthesis of the pentacyanoferrate compounds used to accelerate the production of indophenol. Preparation of the stock reagents is then explained. Finally, the solutions used for the various experiments are reported. In all cases, reagent grade chemicals were used without further purification, except where noted.

1. Synthesis of Pentacyanoferrate Compounds.

The compound aquopentacyanoferrate, AqF, was shown by Patton to be effective in accelerating the production of indophenol. This compound was thus synthesized by the modified procedure of Patton [17] and used during early reaction studies. However, in reviewing the literature of pentacyanoferrate compounds, it was found that the aquo complex was difficult to produce in pure form [47]. One compound used in the study of octahedral iron complexes was sulfitopentacyanoferrate, SpF. The synthesis of this compound is similar to the aquo compound, however, the product is much purer and more stable in aqueous solutions, making it favorable over AqF. The effect of SpF on the Berthelot reaction had not been determined. However, in aqueous solutions, the sulfito group is slowly replaced by an aquo group to form AqF. This suggested that the compound could eventually (if not immediately) accelerate the Berthelot reaction.

The sulfitopentacyanoferrate compound was synthesized by the procedure of Baran and Muller [48] as modified from Hofmann [49]. The 5 M NaOH was prepared by dissolving 10 g NaOH (Columbus Chemical

Industries, Columbus, WI) in 50 mL distilled water. A 40% solution of Na_2SO_3 was prepared by dissolving 40 g of the salt (J. T. Baker Chemical Co., Phillipsburg, N.J.) in 100 mL distilled water. After cooling these solutions, 20 mL of the cold NaOH was mixed with 30 mL of the cold Na_2SO_3. The mixture is placed in an ice bath and 5.5 g of $Na_2[Fe(CN)_5NO]\cdot 2H_2O$ (J. T. Baker Chemical Co.) is added slowly, with stirring. The solution is kept below 10 C for 24 hours. Then cold ethanol is added to precipitate a red-yellow oily resin. It was found that dropwise addition of ethanol near and through the saturation point helped reduce the amount of oily resin and increase the yield of SpF. After decanting off the supernatant liquid, the resin was redissolved with cold distilled water. After complete dissolution of the resin, cold ethanol was slowly added to form a yellow, flaky precipitate. This precipitate was collected by suction filtration and then re-dissolved in cold distilled water. The recrystalization process was repeated a minimum of six times to obtain a pure compound. The canary yellow precipitate was then dried in a vacuum desiccator over concentrated H_2SO_4.

2. Experimental.

The effect of the coupling reagent was tested under experimental conditions similar to previous studies. It was of interest to determine what step of the Berthelot reaction was influenced by the coupling reagent. Because HOCl and NH_3 react to form NH_2Cl so rapidly, it does not seem likely that this step is accelerated by the coupling reagent. To be thorough, the following studies were performed. Hypochlorite

solutions were prepared in the usual manner. Ammonia solutions were prepared to contain the SpF. Concentrations were chosen to provide second-order reaction conditions.

3. Results and Discussion.

Data from these solutions were analyzed using the simplex fitting routine and the same second order reaction model used for the reaction in the absence of SpF. The model closely reproduced the data for each concentration tested. The coupling reagent produced no noticeable effect on the results. Figure 3.9 shows a representative fit for this data. Table 3.5 lists values for k' returned by the fitting routine. Values of k_1 are calculated from k'. The rate constant determined in the presence of SpF was $(3.13 \pm 0.06) \times 10^6$ $\underline{M}^{-1}$ s^{-1}, which is equivalent (within error limits) to the value obtained with SpF absent.

E. CONCLUSION

The reaction has now been studied under various conditions of pH, including the pH range within which the Berthelot procedure for the determination of ammonia is typically done (pH 10-11). A wide range of reagent concentrations was used to allow for analysis under both pseudo-first-order conditions and second order conditions. Data have been collected for both the disappearance of hypochlorite and the appearance of a product. The collected data have been analyzed using

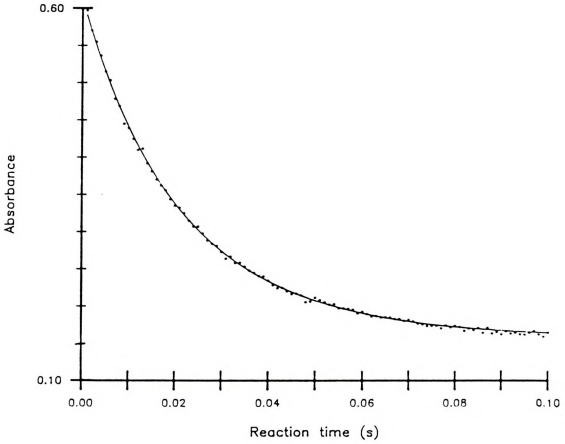

Figure 3.9 Fit of a second-order model to data collected in the presence of the coupling reagent.

TABLE 3.5
Determination of the second order rate constant
(in the presence of coupling reagent)

Soln.#	k′[a]	$k_1 \times 10^{-6}$
1	18,426	3.202
2	18,253	3.172
3	18,400	3.198
4	17,883	3.108
5	17,467	3.036
6	17,872	3.106
7	17,727	3.081
8	18,011	3.130

[a] Values of k′ are determined by a non-linear fit of second order data.

Avg value: $k_1 = 3.129 \times 10^6$
Std. deviation = 5.8×10^4

rate constant: $k_1 = 3.13 \pm 0.06 \times 10^6\ M^{-1}\ s^{-1}$

both linear and non-linear models. The reaction model has fit the data very well in each case.

The reaction order for ammonia has been determined under conditions of excess NH_3 as well as excess Cl_T. In one study N_T was varied by a factor of 7.5 to test the reaction order. All experimental results indicate that the reaction order for NH_3 is 1 and not 0.8. The rate constant has now been determined under conditions employed in the Berthelot procedure (excess hypochlorite). Values for the rate constant have been consistent. The second order rate constant for the first step of the Berthelot reaction is 3.2×10^6 $\underline{M}^{-1}$ s^{-1}. It has been shown that the presence of the coupling reagent has no effect on the rate constant for this reaction step.

CHAPTER IV

THE REACTION BETWEEN MONOCHLORIMINE AND PHENOL

This chapter concerns the second step of the Berthelot reaction. In this step, a reaction occurs between monochloramine and phenol. The studies reported in this chapter were performed, where possible, on the isolated reaction step. The kinetics of the reaction were examined and the effect of sulfitopentacyanoferrate on the kinetics was determined. Finally, the first direct evidence showing the formation of chlorimine as a product of this reaction step and an intermediate in the Berthelot reaction sequence is presented.

A. INTRODUCTION

In the mechanism proposed by Bolleter and co-workers [7], the monochloramine produced in the first step of the Berthelot reaction couples with phenol to produce benzoquinonechlorimine. This product, hereafter referred to as chlorimine, was never isolated or even directly identified by these workers. The only evidence offered to support the formation of chlorimine was the observation that other para-substituted anilines were found to react with phenol to produce a blue color in solution with a spectrum matching that of indophenol. Although there is general acceptance of the Bolleter mechanism for the Berthelot reaction, there is still no direct evidence to show that chlorimine is produced during this reaction.

Examination of the literature reveals that very little has been published concerning the kinetics of this reaction step. Information on the effect of the coupling reagent is also scarce. Patton [16,17] concluded that the compound aquopentacyanoferrate, AqF, acted on NH_2Cl to couple it to phenol. This was based on the observation that mixtures of NH_2Cl, AqF, and an excess of phenol readily form indophenol. Little additional information exists because the reaction between NH_2Cl and phenol is difficult to follow by spectrophotometric methods. Although these reagents absorb in the UV region, phenol exhibits such broad, strong absorption bands that other UV absorbing species are frequently obscured. With molar absorptivity values in the 10^4 $\underline{M}^{-1}$ cm^{-1} range for phenol and the phenolate ion, high absorbance values result for concentrations as low as 10^{-5} $\underline{M}$ phenol. The UV spectra for phenol and phenolate ion are shown in Figure 4.1. Chlorimine, the proposed product of the reaction, exhibits a wavelength of maximum absorbance, λ_{max}, at 287 nm. Although this species also absorbs strongly, its low relative concentration would cause it to be spectrophotometrically obscured by the phenol in solution. NH_2Cl, which absorbs with a λ_{max} at 245 nm, would also be obscured by phenol. The inability to deconvolute the absorption bands explains why information on this reaction is lacking.

B. KINETICS STUDIES

During recent years the ability to collect and store spectral data in digital form has become widespread. High-powered data analysis techniques such as scaling and spectral subtraction have now become

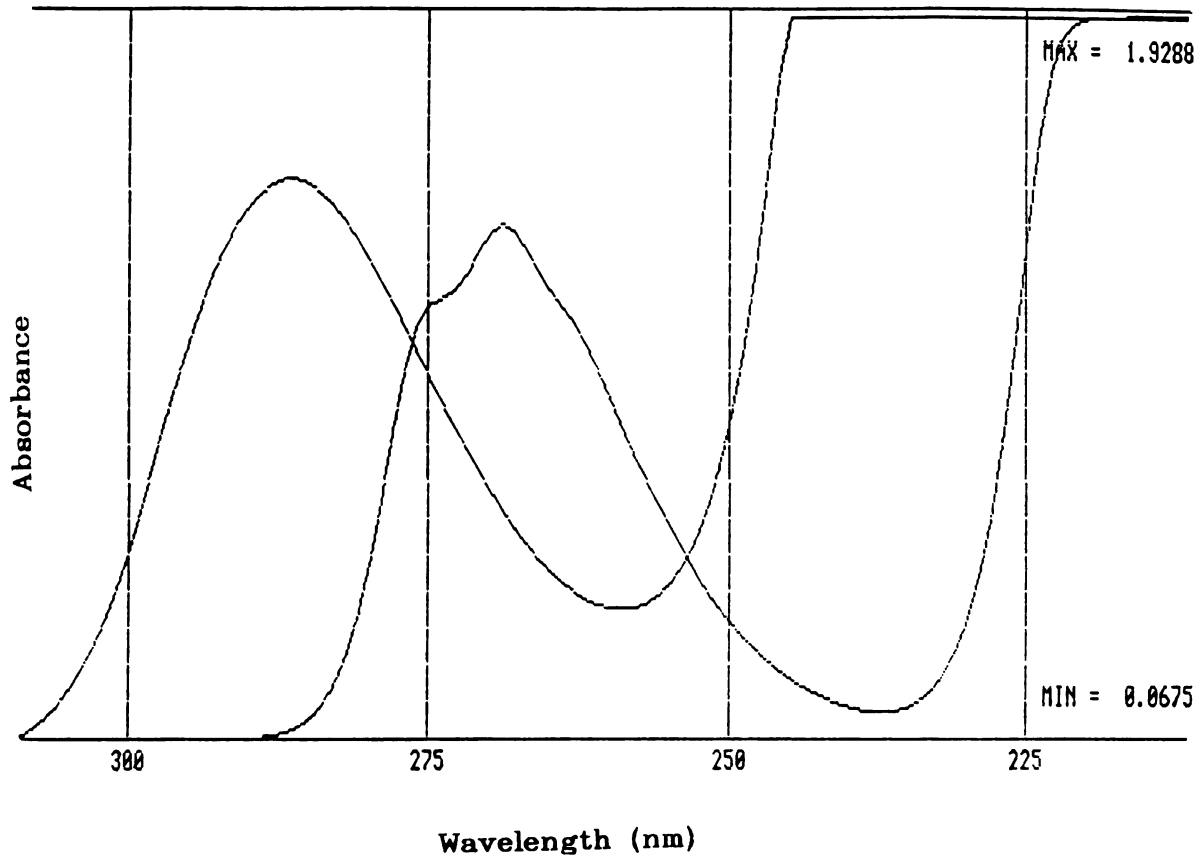

Figure 4.1 Absorption spectra for phenol and phenolate ion. Phenol exhibits a λ_{max} at about 270 nm, while phenolate ion has a λ_{max} at 287 nm.

common. Such techniques aid in the deconvolution of highly overlapped spectra. This ability has been used to aid data analysis in the following studies of the phenol-monochloramine reaction.

1. Reagent Preparation

a. Phenol

A stock solution of phenol was prepared by dissolving the reagent grade solid (Fisher Scientific Company) in distilled water. No further purification of the solid was performed. Solutions of phenol and phenolate were prepared by diluting 1 mL portions of the stock solution in distilled water containing 0.1 N HCl and 0.1 N NaOH, respectively.

b. Synthesis of Monochloramine

Stock solutions of monochloramine were prepared from NH_4Cl (J. T. Baker) by the procedure of Kleinberg [50]. The greatest yield of NH_2Cl was obtained when the synthesis and subsequent back-extraction of product were performed rapidly and when distilled water, buffered to pH 10, was used as the extraction solvent. The concentration of extracted NH_2Cl was determined by thiosulfate titration.

c. Preparation of Sulfitopentacyanoferrate.

The SpF solid was synthesized as described in Chapter 3. Solutions of SpF were prepared by dissolving appropriate amounts of the solid in distilled water.

2. Experimental

Solutions of phenol and NH_2Cl were prepared at various concentrations and were buffered to a constant pH with borate buffer. Spectra were recorded on a Perkin-Elmer Lambda 3 spectrophotometer controlled by a Model 3600 Data Station. Individual UV spectra were recorded for phenol, phenolate ion and NH_2Cl solutions prepared from the stock reagents. For reaction mixtures, solutions were pipetted directly into a 1 cm quartz cell using a digital pipet (Eppendorf). The cell was shaken rapidly and placed in the spectrophotometer. Multiple scans were recorded in the UV region at fixed intervals. Data were stored digitally and preserved on floppy disks for later analysis.

3. Results and Discussion.

a. The Phenol-NH_2Cl Reaction

A mixture of phenol and NH_2Cl, buffered at pH 8, was placed in the spectrophotometer. Spectra were recorded for the mixture at 15 minute intervals for a total of 90 minutes. A final spectrum was recorded 3.5 hours after mixing. This entire process was repeated for a mixture of the two reagents buffered to pH 10. No reaction was evident for the mixtures at either pH; the initial and final spectra were essentially identical. Either the reaction is over before the first spectrum was recorded, or no reaction occurs under these conditions.

The data analysis capabilities of the instrument were used to determine which case was true. The spectrum for phenol was transferred into memory and scaled by the dilution factor of the

reaction mixture. This process was also performed for the spectrum of the NH_2Cl. Both scaled data sets are shown in Figure 4.2, along with the spectrum resulting from addition of the two reagent spectra. The sum of the reagent spectra represents the spectrum of the reaction mixture at t=0 for the reaction. Figure 4.3 shows this same initial reaction mixture spectrum plotted on the same axes as the spectrum recorded from the reaction mixture after 3.5 hours. It is clear that no reaction occurs within the 3.5 hours under these conditions. The equivalent process repeated for the pH 10 reaction mixtures indicates that no reaction occurs at this higher pH.

Patton [16,17] also reported that no reaction occurs between phenol and NH_2Cl in the absence of AqF. This conclusion was based on the lack of formation of indophenol in mixtures of the two reagents. However, the reaction between NH_2Cl and phenol is just an intermediate step in the formation of indophenol. It is possible that a reaction occurred, but that it did not produce indophenol. The absence of indophenol in the solutions is not conclusive proof of the lack of any reaction. In the experiments reported here, the reaction mixture spectrum is shown to be a linear sum of the reagent spectra. This does show that the reagents do not react in any way. In the absence of the coupling reagent, there is essentially no reaction over the pH range 8-10 for reaction times exceeding 3 hours.

b. Effect of SpF on the reaction

The effect of SpF was determined by preparing solutions containing both phenol and SpF. The phenol-SpF mixture was then added to a cell containing NH_2Cl and the spectrum of the mixture was

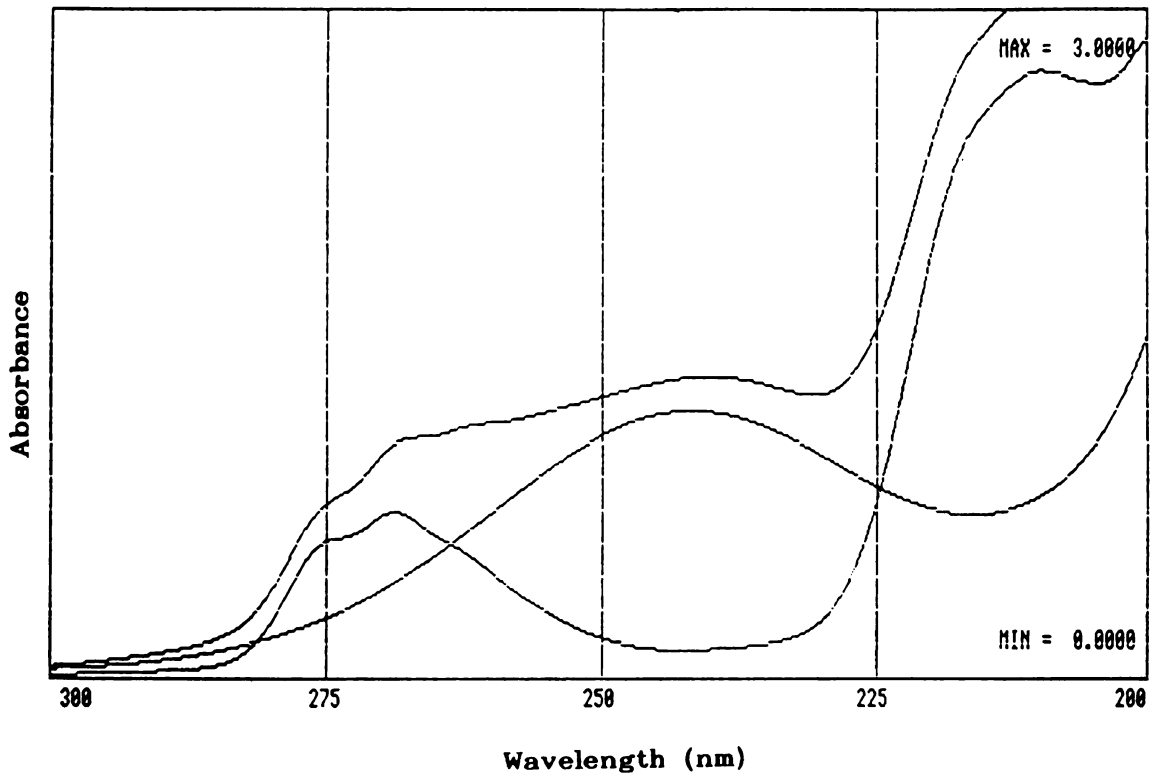

Figure 4.2 Spectrum of phenol, with lmax at 270 nm (lower left), and NH_2Cl, with λ_{max} at 245 nm (lower right). The upper spectrum is the sum of the phenol and NH_2Cl spectra, representing the theoretical spectrum of the reaction mixture at the instant of mixing.

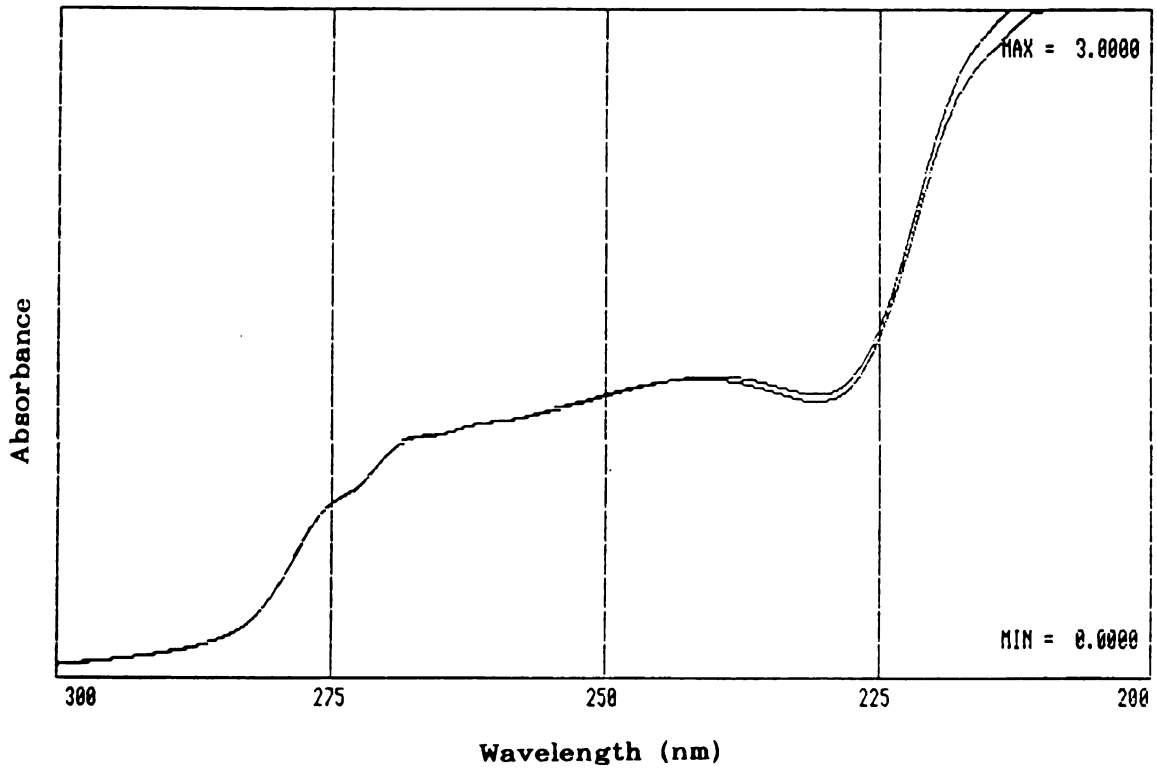

Figure 4.3 Comparison of the theoretical absorption spectrum of a mixture of phenol and NH_2Cl, at t=0, with the experimentally measured spectrum of the pH 8 reaction mixture 3.5 hours after mixing.

recorded from 200-450 nm. Several scans were recorded at about 5 minute intervals. The concentrations of phenol and NH_2Cl used in these solutions were equivalent to the concentrations used in the prior study. The concentration of SpF was 3.7×10^{-4} M, roughly half of the concentration of NH_2Cl. Although the phenol and NH_2Cl concentrations were the same in both studies, the initial reaction spectra bore no resemblance to each other. For reaction mixtures containing SpF, the absorption bands of phenol, NH_2Cl and SpF are obscured or missing. A visible blue color developed within the first 5 minutes and the spectrum developed a major absorption band at 350 nm. The solution also exhibits an absorption band at 635 nm. Both of these peaks have previously been assigned to indophenol. Figure 4.4 shows spectra recorded for the reaction mixture.

In the absence of SpF, the second reaction step of the Berthelot reaction is clearly a rate limiting process. It accounts for the long periods of time required to produce color in Berthelot procedures in the absence of coupling reagents. In the presence of SpF, the reaction proceeds at a greatly accelerated rate and continues through the third reaction step of the Bolleter mechanism [7] to produce indophenol. Since the indophenol absorption band obscures the reagent absorption bands, and since the kinetics of the third reaction step are not completely known, it is not yet possible to determine the kinetics of the second reaction step when SpF is present. It is, however, clear that the SpF (and other such coupling reagents) act directly on this step of the Berthelot reaction sequence to accelerate the formation of a precursor which ultimately produces indophenol.

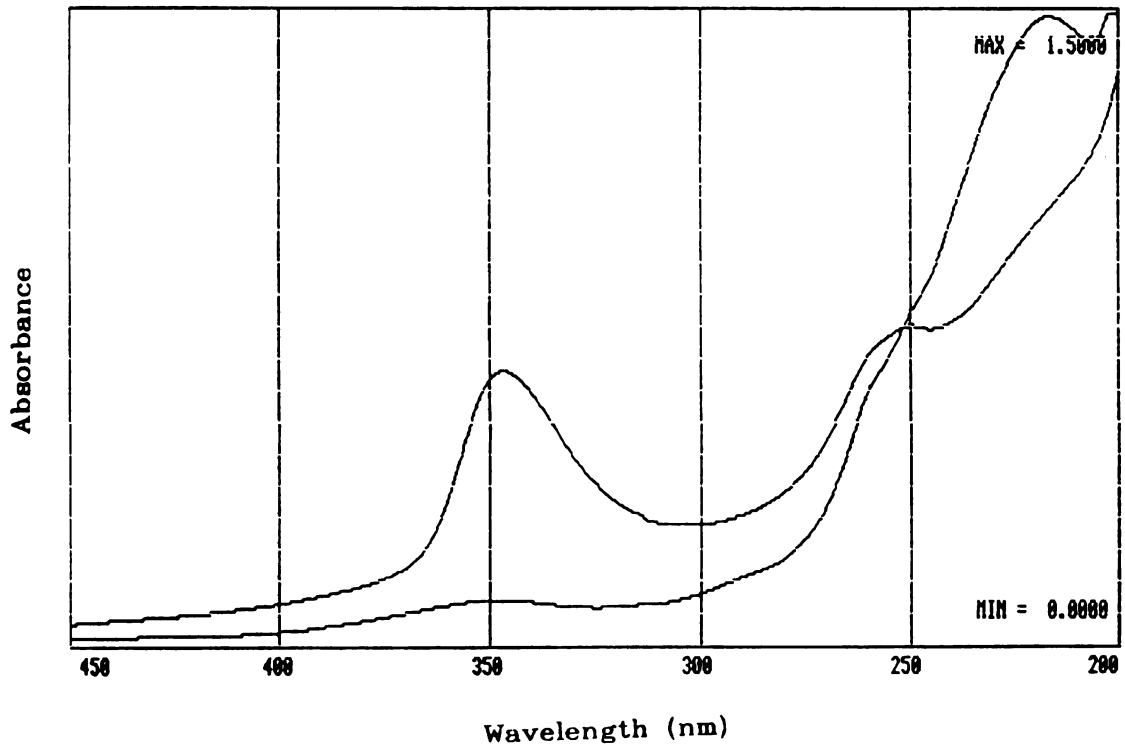

Figure 4.4 Spectra for a reaction mixture of phenol, NH_2Cl and SpF shortly after mixing (lower) and after a 5 minute interval (upper).

C. REACTION PRODUCT STUDIES

The high degree of overlap of the absorption bands of the reagents in the second step of the Berthelot reaction makes it difficult to determine if chlorimine is being produced in the reaction. In the synthesis of NH_2Cl, diethyl ether is used to extract the NH_2Cl and the reagent is then washed back into aqueous solution for further use. Such a technique could be used to isolate the product of the second reaction step. Once isolated, spectrophotometric techniques could be used to identify the product. The following study details this process.

1. Synthesis of Chlorimine

A commercial source for this air and light sensitive compound was not found. It was thus synthesized from p-aminophenol (Fisher Scientific Company) by the procedure of Baran and Muller [48]. Since the p-aminophenol itself is light-sensitive and unstable, it was first purified by filtering a hot aqueous solution through activated carbon and then cooling and recrystallizing the compound from distilled water. The resulting white crystals were used to synthesize chlorimine through a reaction with sodium hypochlorite. The filtered, dried chlorimine solid was purified by recrystallization from ether. The resulting yellow needles had a melting point of 85.6 C, in agreement with the literature. The IR spectrum of the compound confirms the presence of the correct functional groups and mass spectral analysis indicates a parent peak at the correct m/z ratio. The chlorimine was stored in a desiccator in the dark until needed. The solid was stable for several weeks when so

stored. Additional chlorimine was prepared whenever the yellow crystals developed a green-tinted hue indicative of decomposition.

2. Experimental

The absorbance of phenol was measured in the Perkin-Elmer spectrophotometer at 270 nm. Then 5 mL of the phenol were added to a 10 dram vial containing 5 mL N-heptane. The vial was covered and shaken. The aqueous phase was removed and the absorbance was measured at 270 nm to determine the amount of phenol extracted. This same procedure was repeated for the phenolate solution by measuring the absorbance at 287 nm before and after shaking with an equal volume of N-heptane.

Solutions of chlorimine and SpF were prepared by dissolving a few mg of each solid in distilled water. Distribution ratios were determined for these compounds by measuring the absorbance at 286 nm and 440 nm, respectively, both before and after extracting with equal volumes of N-heptane.

Monochloramine solutions prepared by the procedure of Kleinberg [50] were found to contain small amounts of ether. Ether is very soluble in N-heptane and could possibly distort the distribution ratio. For these studies, monochloramine was prepared as follows. Several mL of an NH_4Cl solution were added to a 10 dram vial containing 5 mL of N-heptane. A limiting amount of sodium hypochlorite was placed in the vial and the mixture was shaken thoroughly for several minutes. The organic phase was removed and the aqueous phase discarded. The spectrum of the organic phase was recorded from 320-230 nm. An

absorption band for NH_2Cl was present and the absorbance at λ_{max} was determined. Then 4 mL of the organic phase were shaken with 1 mL of distilled water. The organic phase was removed and the absorbance was again measured at λ_{max}.

3. Results and Discussion

By applying Beer's Law to the absorbance data collected, distribution ratios can be determined for chlorimine and for the reagents in the reaction between NH_2Cl and phenol. The concentration distribution ratio, D_c, is given by $D_c = [C]_o/[C]_w$. The subscripts o and w indicate organic phase and water, respectively, and C represents the species being determined. The measured quantities are the initial absorbance, A_{tot}, and the absorbance after extraction, A_e. It can be shown that for extraction from water, $D_c = (A_{tot}-A_e)/A_e$. When the extraction is from N-heptane to water, D_c is simply the reciprocal of the above. An aqueous solution of chlorimine having an absorbance of 0.407 at 287 nm was found to have an absorbance of 0.088 after extraction with N-heptane. The calculated distribution coefficient is thus 3.62. Table 4.1 lists distribution ratios calculated for the tested compounds. As can be seen, ionic species are not extracted into N-heptane. Of the neutral species chlorimine, phenol and NH_2Cl, only chlorimine is preferentially extracted into N-heptane. It should thus be possible to extract into N-heptane any chlorimine produced in the reaction between phenol and NH_2Cl. Any phenol and NH_2Cl which might be extracted along with the chlorimine could be washed back into an aqueous phase with water.

TABLE 4.1
Distribution Ratios
Between Water and N-heptane

Chemical species	Extracted from	A_{tot}	A_f	D_c
chlorimine	water	0.407	0.088	3.6
phenol	N-heptane	1.177	0.137	0.132
phenolate	water	0.988	0.987	ns
SpF	water	0.635	0.635	ns
indophenolate	water	0.742	0.742	ns
monochloramine	N-heptane	0.302	0.066	0.28

A_{tot} is the absorbance at λ_{max} in the indicated phase before extraction.

A_f is the absorbance at λ_{max} for the same solution after extraction.

ns indicates species non-soluble in n-heptane.

Figure 4.5 shows a spectrum of chlorimine dissolved directly in N-heptane. The spectrum exhibits the same general shape as the aqueous chlorimine spectrum, with the exception that the absorption band is shifted to a smaller wavelength by 5-7 nm. This shift in λ_{max} is consistent with shifts observed for NH_2Cl and phenol in N-heptane. The spectrum of chlorimine extracted from an aqueous phase into N-heptane was identical to that of Figure 4.5. The extraction thus does not alter the compound.

It now remained to extract the product of the second step of the Berthelot reaction while the reaction was progressing. A solution of NH_4Cl buffered to pH 10.7 was placed in a 20 dram vial. To the vial were added, in succession, excess phenol, SpF and sodium hypochlorite. The vial was closed and shaken to initiate the reaction. When a faint blue color was visible in the aqueous phase, 6 mL of N-heptane were added to the vial. After shaking together for several minutes, the organic phase was removed from the vial and placed in a cell. The absorbance of the organic phase was recorded from 320-230 nm, as shown in Figure 4.6. Two absorption bands are evident. The major band consists of three peaks, while a minor absorption band appears as a shoulder in the vicinity of 285 nm. The organic phase was removed from the cell and shaken with a few mL of distilled water. The spectrum of the washed organic phase was recorded and stored. This process was repeated using a second distilled water wash. The spectrum of the final organic phase is shown in Figure 4.7 along with the two spectra recorded earlier. As can be seen, the major peak in the original organic phase was preferentially extracted from the N-heptane, leaving behind what was originally the shoulder. The

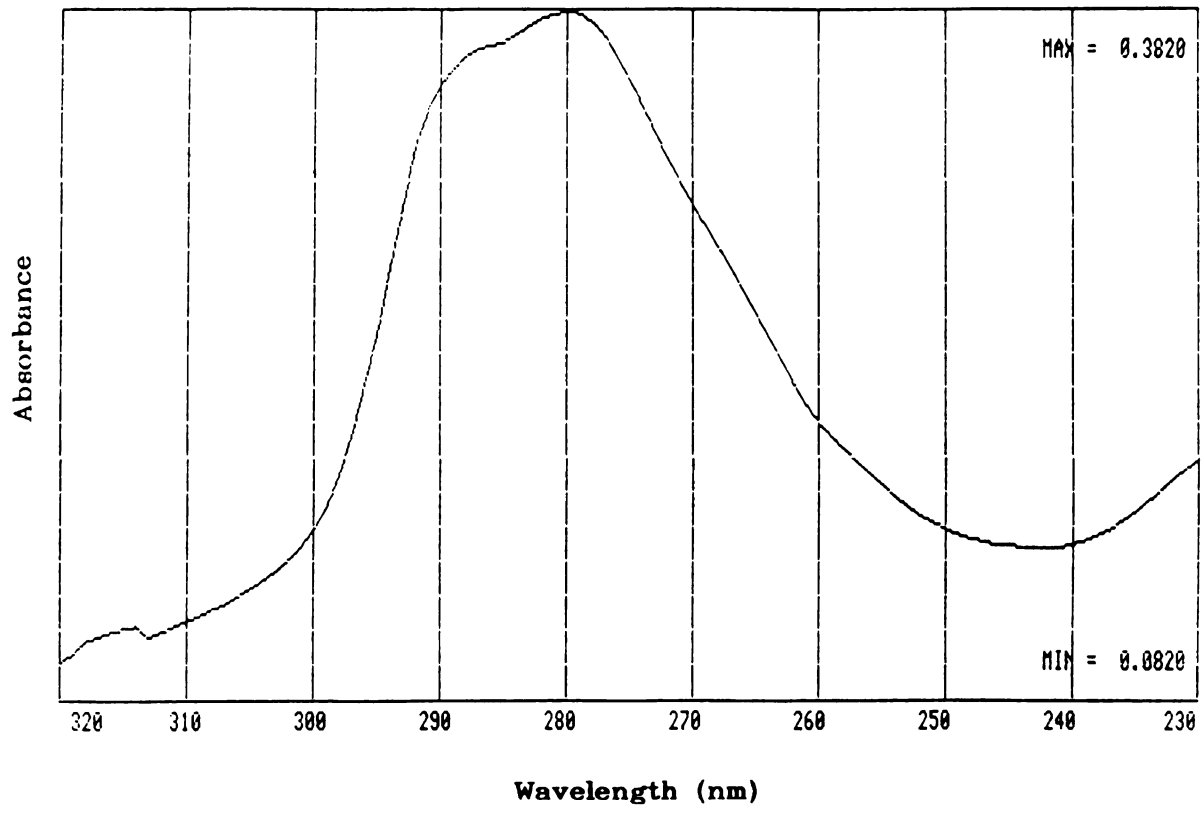

Figure 4.5 Absorption spectrum of chlorimine in N-heptane. The λ_{max} for chlorimine is 280 nm in this solvent.

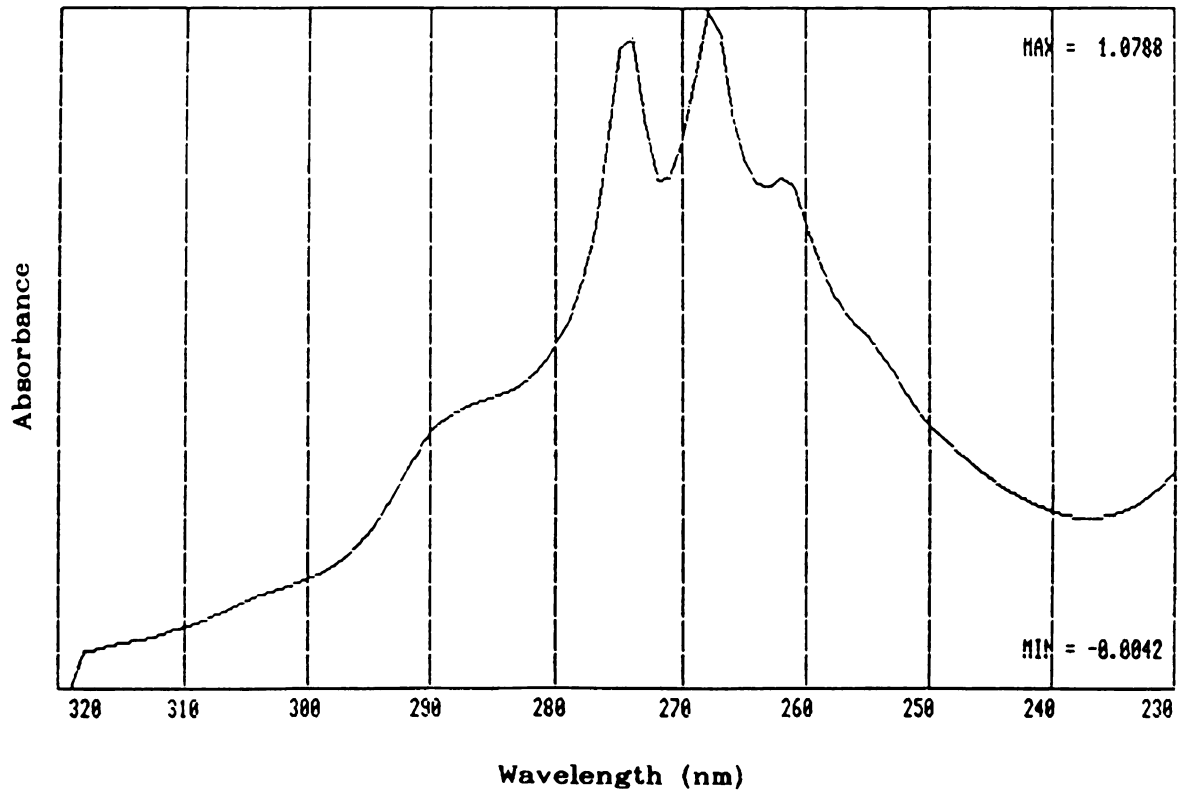

Figure 4.6 Spectrum of an N-heptane extract of an aqueous mixture of HOCl, NH_3, SpF and phenol. Indophenol was being produced in the aqueous phase at the time of the extraction.

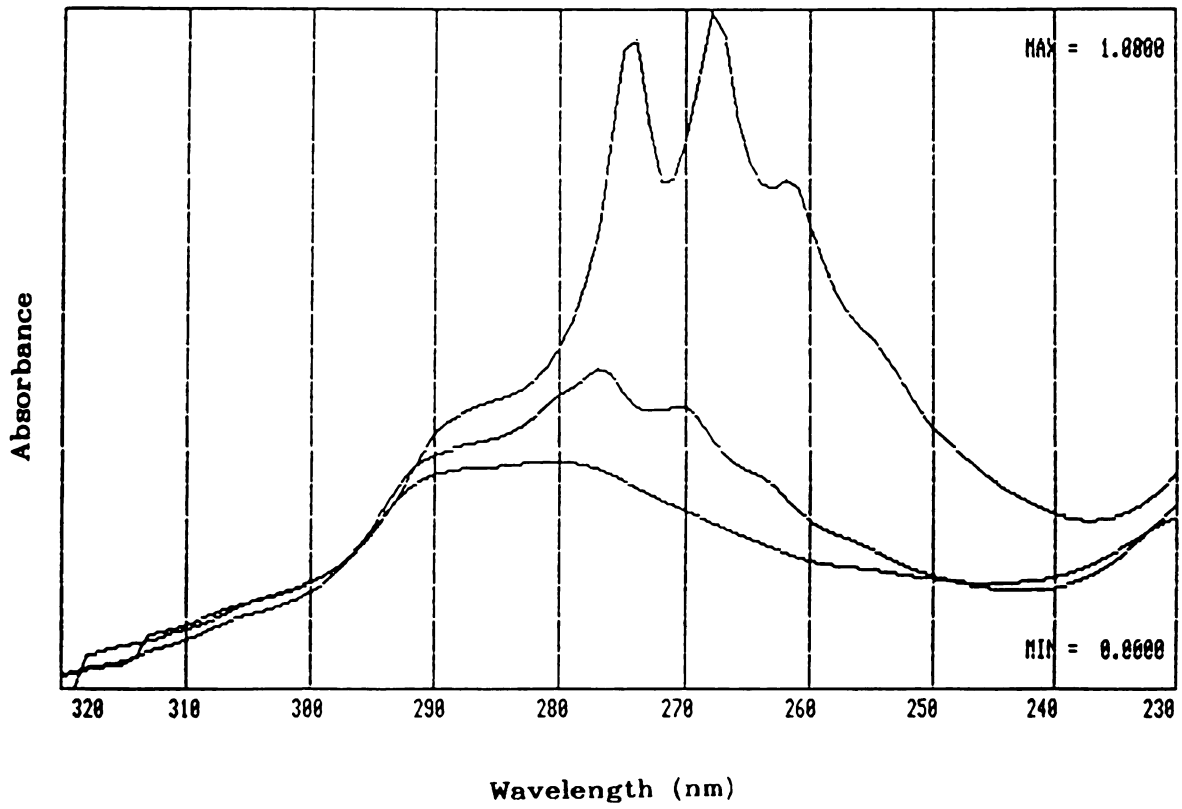

Figure 4.7 Spectrum of an N-heptane extract of a Berthelot reaction mixture (upper spectrum) and the same N-heptane phase after two successive washes with an equal volume of water (lower two spectra). The species responsible for the triplet band is rapidly extracted back into water, leaving behind a species with a λ_{max} at about 280 nm.

spectrum of the N-heptane extract after the final aqueous wash is shown in Figure 4.8. The spectrum of chlorimine dissolved in N-heptane is also shown in Figure 4.8. The agreement between the two spectra identifies the minor absorption band of the original extract as chlorimine. This evidence shows that chlorimine is indeed formed in the reaction between phenol and monochloramine.

It was also of interest to identify the compound responsible for the three peaks observed in Figures 4.6-4.7. The distribution studies performed previously indicate that the absorption band is not due to SpF, phenolate, or indophenolate. The band is also not due to NH_2Cl, which absorbs at 250 nm in N-heptane. The other major species in the original reaction mixture were NH_3 and OCl^-. Although the reaction mixture was buffered to pH 10.7, a small amount of undissociated phenol was also present in the mixture. Finally, yet unknown reaction products could be responsible for the absorption band. The band is most likely due to phenol, which absorbs in the same region as the observed three peaks. To verify this, a solution of phenol was adjusted to pH 10.7 with 0.1 N NaOH and shaken with N-heptane. The organic phase was removed and the spectrum of the N-heptane phase was recorded. The resulting spectrum exhibited an absorption band with the same three-peak shape. The spectrum is shown in Figure 4.9 along with the spectrum of the original extract of the reaction mixture (Figure 4.6). It can be concluded that the observed band results from the extraction of phenol from the original reaction mixture. As indicated by the distribution ratios of Table 4.1, phenol should extract back into an aqueous phase preferentially over chlorimine. This was shown to be the case in Figure 4.7. This back extraction of phenol leaves behind chlorimine, which is

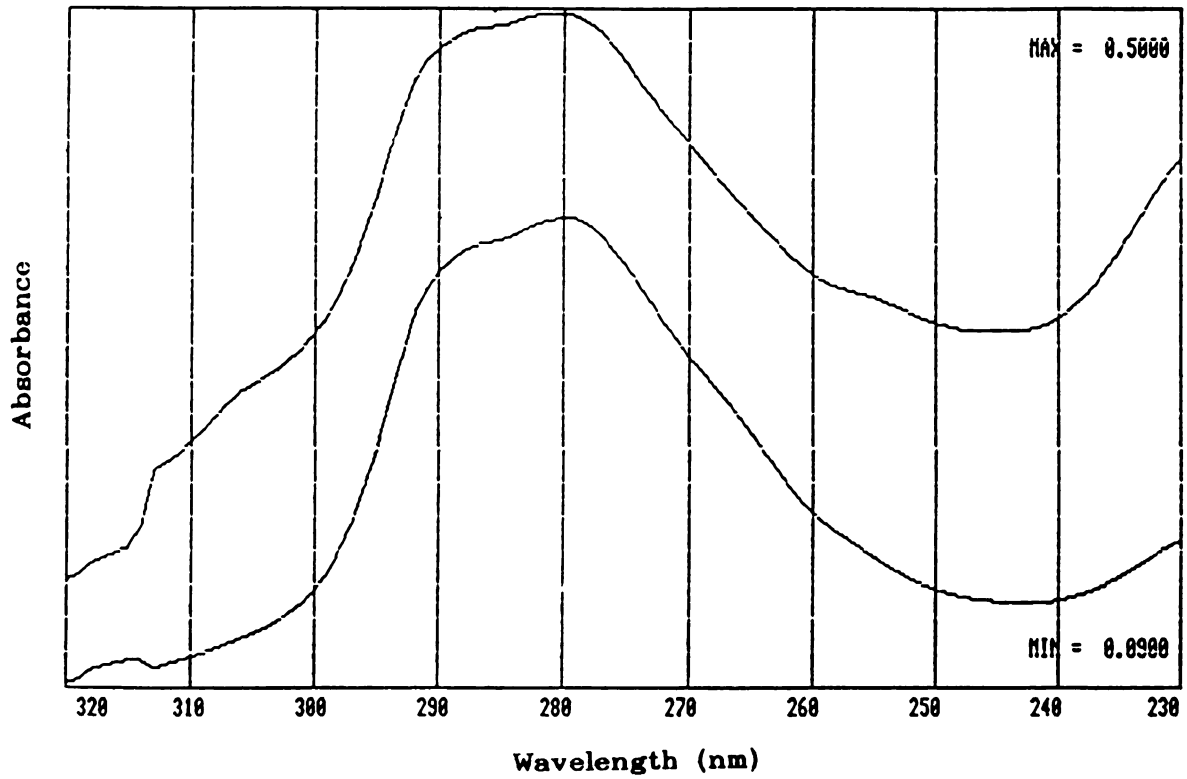

Figure 4.8 Comparison of the spectrum of chlorimine in N-heptane (lower curve) with the spectrum obtained by extracting and isolating an intermediate from an aqueous solution undergoing the Berthelot reaction. The solutions are not of equal concentration.

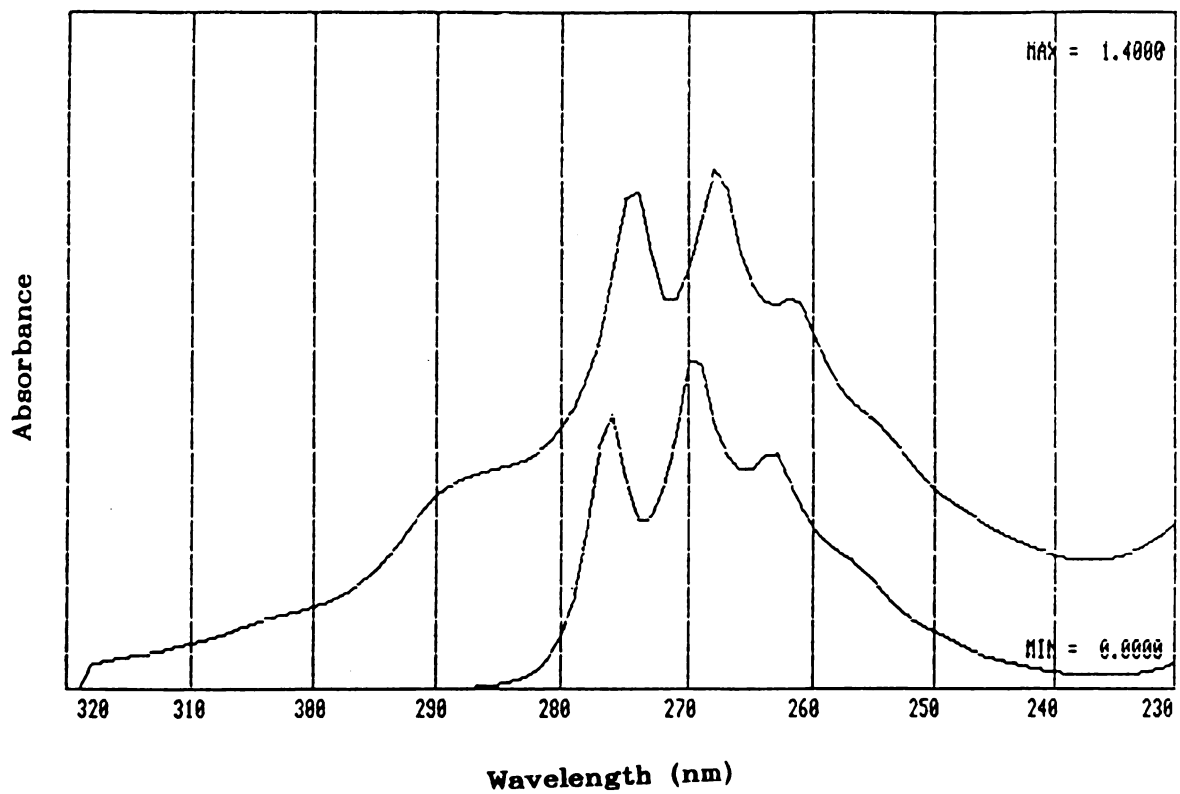

Figure 4.9 Comparison of an N-heptane extract of an aqueous Berthelot reaction mixture (upper curve) with an N-heptane extract of phenol from a solution containing predominantly phenolate ion.

easily identified in the N-heptane phase. This represents the first direct evidence of the formation of chlorimine in the Berthelot reaction sequence.

CHAPTER V

THE REACTION BETWEEN QUINONECHLORIMINE AND PHENOL

As shown in the previous chapter, chlorimine is produced as a result of the second step of the Berthelot reaction. This chapter presents details on the aqueous chemistry of chlorimine and its reaction with phenol. These two compounds react to form indophenol, the final product in the Berthelot reaction. Studies of the reaction of phenol with phenolamines and -imines are first reviewed. Although no previous studies were found involving chlorimine, the reviewed works on related compounds provide useful insights into reaction studies presented in this chapter. The synthesis of chlorimine is then described, followed by studies of its stability. Reaction kinetics for the formation of indophenols from these compounds is reported. Finally, the effect of the coupling reagent on the rate of the reaction is examined. Benzoquinonechlorimine will again be specifically referred to in this chapter as chlorimine.

A. HISTORICAL

Although reactions producing intensely colored indophenols had been known for decades prior [51], the condensation of quinoneimines with phenol to produce indophenol was first described by Hirsch in 1880 [52]. This reaction formed the basis of a procedure for the determination of phenols published by Gibbs in 1927 [53]. He reported

that precise quantitative information could be obtained by reacting phenols with a saturated solution of 2,6-dibromoquinonechlorimine, Br_2Q. He claimed a sensitivity of 0.05 ppm for phenol using his method. Gibbs also reported that the rates of these reactions were highly pH dependent. He found that quinoneimines decomposed in aqueous solutions, but he did little more than note that it occurred slowly.

In a subsequent paper published later that year, Gibbs [54] investigated the mechanism for the reaction between phenol and Br_2Q. The reaction was found to involve the phenolate ion, whose pH dependence explains the previously noted pH effect [53]. In buffered solutions containing an excess of phenol, the reaction between phenol and Br_2Q follows a pseudo-first-order rate law. The second order rate constant, calculated from the first-order data, was determined to be 2.72×10^2 $\underline{M}^{-1}$ s^{-1} at 20 C. The rate of hydrolysis of Br_2Q was also found to be pH dependent. This rate increases as the hydroxyl ion concentration increases. However, in the presence of a large excess of phenol, hydrolysis was found to be insignificant in comparison to the rate of formation of indophenol.

In 1954, a report by Kulberg and Borzova [55] on the specific determination of chlorine indicated that phenolamines readily react with phenol to form indophenols. The suggested mechanism involves oxidative conversion of the phenolamine to a phenolimine by chlorine. The imine which is produced then couples with phenol to form indophenol; hence p-aminophenol is oxidized by chlorine in acidic media and undergoes subsequent coupling with phenol to form indophenol. A procedure was described for the quantitative determination of chlorine using aniline and phenol. The kinetics of these reactions were not investigated.

Results of a study of the hydrolysis of benzoquinone mono- and di-imines were published by Tong in 1954 [56]. Because these imines are unstable, they were generated *in situ* by oxidizing the appropriate phenolamines with ferricyanide. Tong found that hydrolysis of quinoneimine produces benzoquinone, while hydrolysis of the di-imine first produces the mono-imine, which itself subsequently hydrolyzes to form benzoquinone. Although the imines produced by the action of ferricyanide are in equilibrium with their corresponding phenolamines, the position of this equilibrium during the reaction was not studied. Tong just assumed that the conversion was complete.

In 1969 Corbett [57] reported results of a study of the effect of pH on the *in situ* generation of mono- and di-imine from their respective phenolamines. He confirmed that two moles of oxidant were required to convert one mole of a phenolamine to its corresponding imine. This is consistent with two successive 1 electron oxidation steps. He also found that ferricyanide oxidation of a phenolamine to a phenolimine appears to occur at a diffusion-controlled rate. Corbett found that the equilibrium position of this redox reaction was pH dependent. He determined that quantitative *in situ* generation of quinoneimines occurs only above pH 8. The redox system was found to be unsuitable for kinetics studies in the pH range 4.5 to 7, since color-forming side reactions involving the amine and the imine can occur in this range [57].

Results of a study of the hydrolysis of quinone mono- and di-imines were also reported by Corbett in 1969 [58]. The kinetics of the hydrolysis reaction were found to be first order over the pH range 2-10. He, too, found that hydrolysis of quinoneimine produces benzoquinone. The rate of this hydrolysis was determined to be pH

dependent, increasing as the pH increased. Hydrolysis occurs for both the free imine and its protonated form. The protonated form was found to be 1800 times more reactive than the free imine with respect to hydrolysis.

A report of the study of the kinetics and mechanism of imine reactions with phenols was published by Corbett in 1970 [59]. He concluded that indophenol was produced in two successive steps. The rate-controlling step involves electrophillic coupling of the imine to the phenol to form a leuco-indophenol. The second step is a rapid oxidation of the leuco-indophenol to indophenol by a second molecule of the imine. This second imine is reduced to the original phenolamine during the reaction. Oxidizing agents such as ferricyanide can also oxidize the leuco-indophenol to indophenol. Thus, Corbett determined that aminophenol reacts with phenol and with four molar equivalents of ferricyanide to produce indophenol. Both neutral and ionic forms of the imine are reactive [59]. Rate constants for both reactive forms were determined for the reaction of quinoneimine with 2,6-xylenol. Rate data were also determined for reactions between several substituted phenols and imines. Chlorimine was not included in any of these studies.

In 1977, results of a study of the reaction of phenols with 2,6-dichloroquinonechlorimine, Cl_2Q, were published by Svobodova and co-workers [60]. They determined that, in the absence of other reactants, Cl_2Q decomposed to form products in successive steps. At pH 8.5, complete hydrolysis of Cl_2Q to 2,6-dichloroquinoneimine occurred within two hours. They were surprised to find that this hydrolysis product reacted quantitatively with phenol to produce an indophenol equivalent to the one produced by the parent Cl_2Q. Furthermore, they

found that it reacted with phenol at a faster rate than did Cl_2Q. However, 2,6-dichloroquinoneimine itself slowly decomposed to form a product which did not react with phenol.

At high pH values, Svobodova [60] found that the rate of hydrolysis of both Cl_2Q and 2,6-dichloroquinoneimine increased. Cl_2Q was rapidly converted to the non-reactive product. Spectral and chromatographic techniques were used to identify the products in these studies. No kinetics results were reported for any of these reactions.

A subsequent paper by these workers appeared in 1978 [61]. They concluded that no direct reaction occurred between phenol and 2,6-dichloroquinonechlorimine, despite the fact that there was evidence for this reaction in their earlier study. However, they found no evidence in their reaction mixtures for the reduced form of 2,6-dichloroquinonechlorimine, which Corbett [58] suggested should form during the production of indophenol. After studying the stability of the reagents involved, they reported some optimum conditions for the formation of indophenol from phenols and quinoneimines.

B. KINETICS STUDIES

Reactions between phenols and quinoneimines have been investigated qualitatively and in some cases quantitatively [58-59]. However, the reaction of chlorimine with phenol has not been fully investigated. The following section presents results of a study of this final step of the Berthelot reaction.

1. Reagent Preparation.

a. Chlorimine

Chlorimine was synthesized by the procedure of Baran and Muller [48], as reported in Chapter 4. Stock solutions of chlorimine were prepared by dissolving appropriate amounts of the solid in distilled water in a volumetric flask. The solubility of this compound is low and it dissolves slowly. Since it also hydrolyzes, reagent solutions were prepared and used as rapidly as possible. To aid dissolution, chlorimine was often first dissolved in about 1 mL of ethanol. After dissolution, the chlorimine was buffered at the desired pH with borate buffer and then diluted to volume with distilled water.

During slow kinetics studies, stock solutions of chlorimine were buffered at pH 8 and kept refrigerated. Reagent solutions were prepared from the stock solution just prior to use in order to minimize decomposition due to hydrolysis.

b. Phenol

Stock solutions of phenol were prepared by dissolving the solid in distilled water or in a few mL of ethanol followed by dilution with water. The reagent grade solid was used with no further purification. For pseudo-first order studies, phenol concentrations in the mM range were required. This presented a special problem for studies concerning the effect of pH on the reaction kinetics. It was not possible to prepare mM concentration phenol solutions which were also buffered from pH 8 to pH 11 from a single stock solution of phenol. Instead, stock solutions of phenol were prepared from a single concentrated phenol solution.

Borate buffer was used to dilute each phenol solution such that each was 'buffered to a nominal pH' in the range of 8-11. Reagent solutions of phenol were then prepared by diluting each 'nominally buffered' stock solution to volume with borate buffer of the desired pH. This buffering procedure was found to be sufficient to maintain a constant pH during the reactions so studied.

2. Experimental

Initial experiments on the stability of chlorimine were done using a Perkin-Elmer Lambda 3 spectrophotometer with a Model 3600 Data Station. Solutions of chlorimine were prepared in the 10^{-5} M range and were buffered to a specific pH with borate buffers. The UV spectra were recorded over the range 200-300 nm and stored in digital form. Successive scans were recorded at regular intervals over a period of several hours. Because the sample compartment could not be thermostated, it was opened between scans to prevent excessive heating of the solutions. After all scans were completed, the stored data were plotted together on the same axes to produce a series of time-dependent reaction spectra.

Since the Perkin-Elmer was not equipped to analyze kinetics data, fixed-wavelength studies were performed using a Heath Model EU-701 series spectrophotometer. The instrument was used to collect absorbance data as a function of time for both the hydrolysis of chlorimine and its reaction with phenol. Data were collected at programmed intervals using an IBM data acquisition board (IBM Instrument Corp.) under the control of a personal computer (Bentley

Computer Products). Data were stored in digital form and analyzed using programs developed for the PC. Alternately, data were transferred to a DEC PDP 11/23 minicomputer for analysis.

In many cases the reaction kinetics studied were very slow. It became necessary to monitor the absorbance for upwards of one hour. Analysis times shorter than this did not provide sufficient changes in absorbance for the data to be analyzed with any accuracy. Because the Heath spectrophotometer could not correct for drift in the UV lamp during such long reaction times, spectral data were collected using a double-beam Perkin-Elmer Hitachi 200 spectrophotometer. Initially, the data were recorded on a strip-chart recorder. Eventually, the microcomputer described in Chapter 2 was connected to the output of the spectrophotometer. The microcomputer was programmed to collect absorbance data from the Hitachi and the data were stored in digital form for later analysis.

3. Results and Discussion

a. Hydrolysis

Before proceeding with studies of the reaction between chlorimine and phenol, studies were performed to determine the stability of chlorimine in aqueous solutions of various pH. Quinoneimines are known to hydrolyze [53,54,57-9], and the rate at which they do so can be critical. Not only will hydrolysis change the initial concentration of stock reagents, it produces compounds in solution which may affect the reactions being studied. Figure 5.1 shows time-dependent spectra of chlorimine solutions buffered to different pH values. Figure 5.1a shows

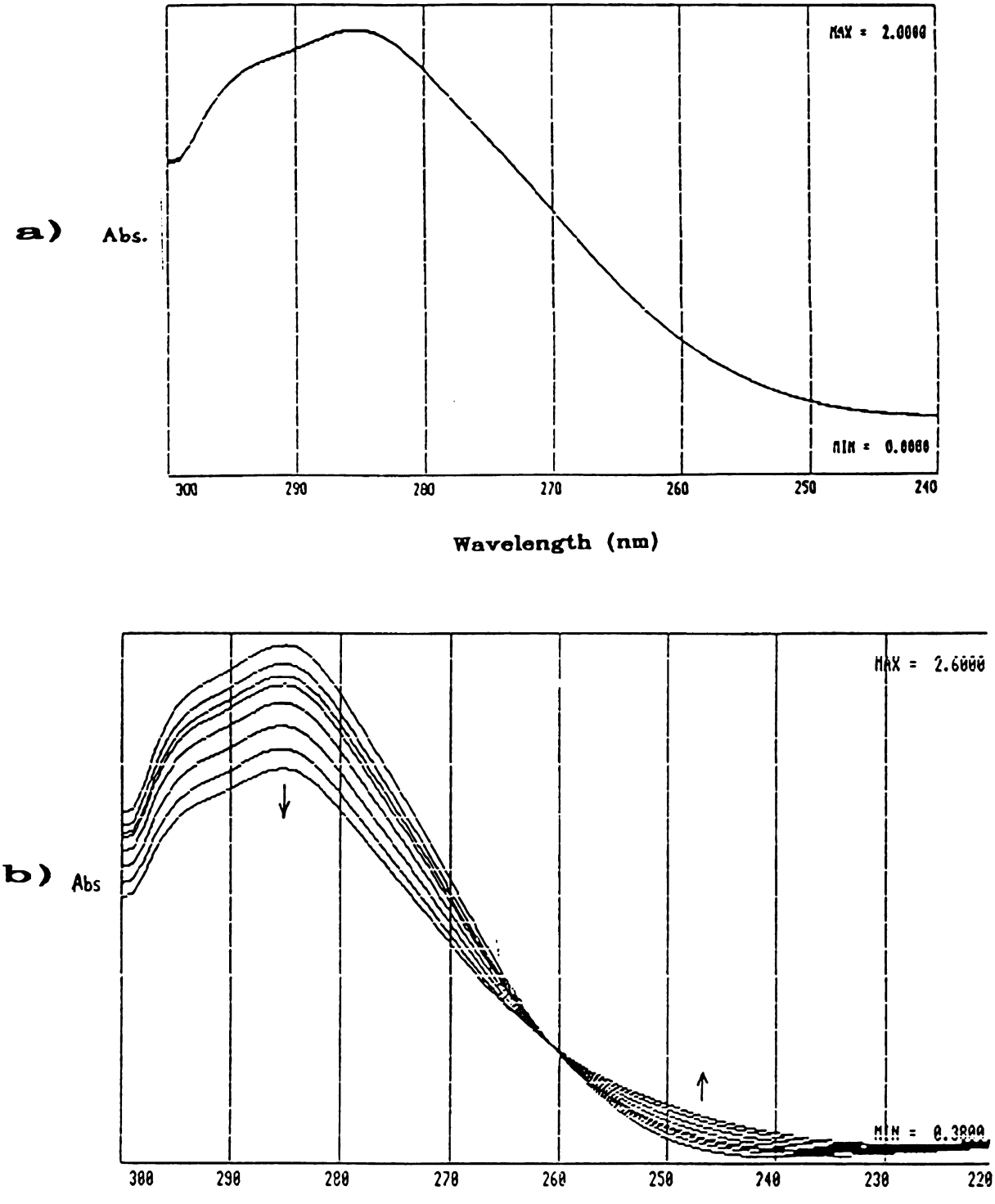

Figure 5.1 a) Time-dependent spectra of an aqueous chlorimine solution at pH 8. The figure consists of multiple spectra recorded over a one hour interval. Slight broadening of the curve indicates that the compound is fairly stable under these conditions.
b) Time-dependent spectra of a chlorimine solution at pH 10. Spectra were recorded over a four hour interval.

spectra recorded for a solution buffered at pH 8. The spectra were recorded at periodic intervals over the course of one hour. The individual spectra are plotted on the same axes. There are only slight changes in the spectra during the one hour interval. Whether this is due to instrumental drift or to actual chemical changes in the solution is uncertain. However, the change is essentially negligible; the absorbance change at λ_{max} is less than 1%.

Figure 5.1b shows spectra recorded at periodic intervals for a chlorimine solution buffered to pH 10. Spectra were recorded at roughly 30 minute intervals for 4 hours. Each spectrum still has the characteristic chlorimine shape, with λ_{max} at 285-287 nm. However, hydrolysis is evident even within the first 30 minutes. The absorbance near λ_{max} continues to decrease during successive scans, while the absorbance in the region of 240-250 nm increases. An isosbestic point for the hydrolysis is apparent at 261 nm, indicating that the hydrolysis leads to a single product.

Hydrolysis of chlorimine is thus a pH-dependent process, with the rate of hydrolysis increasing as the solution alkalinity increases. This pH-dependence is typical of substituted quinonehaloimines [53,54,57-9]. Although none of the previous studies involve an investigation of the hydrolysis kinetics of chlorimine, Svobodova and co-workers [60] did find that ethanolic solutions of 2,6-dichloroquinonechlorimine are stable for over six months when stored in a refrigerator. This suggests that aqueous solutions of chlorimine might also be stable when stored in the cold.

To test this idea, 4.8 mg of chlorimine were dissolved in pH 8 borate buffer and diluted to 50 mL in a volumetric flask. A 1 mL

portion of this stock solution was then diluted to 25 mL. The absorbance of the diluted solution was recorded as 0.574 at 286 nm. The stock solution was refrigerated overnight. After over 26 hours, a second 1 mL to 25 mL dilution of the chlorimine gave an absorbance of 0.566 at 286 nm. Assuming dilution and instrumental errors are negligible, the change in absorbance indicates a chlorimine concentration change of 1.4% during the 26 hours. This greatly enhanced stability makes it possible to prepare stock solutions of chlorimine and to use them to prepare reagent solutions over the course of several hours with negligible changes in the stock concentration. Experiments involving slow kinetics can thus be studied without the necessity of preparing fresh reagents for each concentration to be tested.

This stability facilitated studies of the rate of hydrolysis of chlorimine (at a fixed pH) as a function of the initial concentration. A 1.07×10^{-3} M stock solution of chlorimine, buffered at pH 8, was prepared and refrigerated. One mL of this stock solution was mixed with 15 mL of pH 10 borate buffer and diluted to 25 mL with distilled water. A solution aliquot was added to a spectrophotometric cell and the absorbance was monitored at 286 nm as a function of time. Absorbance data were then collected for a second aliquot of the stock chlorimine solution which had been treated in the same manner. Similarly, the change in absorbance with time was recorded for successively smaller aliquots of the stock chlorimine solution.

Previous workers indicate that hydrolysis of quinoneimines is a first order process [54,59]. A plot of the initial rate vs. the initial concentration of chlorimine should then result in a line with a slope equal to the observed rate constant. Initial reaction rates were

determined through linear-regression analysis of the initial reaction curves of each of the collected data sets. Table 5.1 lists results from the analysis of the data. Figure 5.2 shows a plot of the initial rate versus. the initial chlorimine concentration. The plot is linear despite the low S/N ratio for the data. From the slope of the line, the rate constant for hydrolysis was determined to be 3.8×10^{-6} s^{-1} (2.3×10^{-4} min^{-1}) at pH 8.

An additional series of experiments was performed to determine the rate of hydrolysis as a function of pH. A chlorimine stock solution was prepared by dissolving 3.7 mg of the solid in 1 mL of ethanol in a 25 mL volumetric flask. After adding 5 mL of pH 8 borate buffer, the solution was diluted to volume with distilled water. Reagent solutions were prepared from the refrigerated stock solution by diluting 1 mL aliquots of the stock to 25 mL with distilled water and borate buffer of various pH values. As soon as each reagent solution was prepared, it was placed in the Heath spectrophotometer and the absorbance was monitored at 286 nm. Initial reaction rates were determined by linear-regression analysis of the data. A similar procedure was followed to collect data using the double-beam Perkin-Elmer Hitachi 200 spectrophotometer. Data from this instrument were recorded on a strip-chart recorder. For this first order hydrolysis reaction, the observed rate constant can be calculated as the initial rate divided by the initial concentration of chlorimine. Table 5.2 list results from these experiments. Also included in Table 5.2 are data collected at a later time when the output from the Hitachi 200 spectrophotometer was connected to the microcomputer. This configuration allowed the data to be stored and analyzed in digital form. Figure 5.3 shows a plot of k_{obs}

TABLE 5.1
Hydrolysis of Chlorimine

Solution #	$[Chlorimine]_o$ M x 10^5	$(Rate)_o$ A s^{-1} x 10^5
1	0.859	-0.0611
2	1.29	-0.15
3	1.29	-0.167
4	2.15	-0.17
5	3.01	-0.384
6	3.65	-0.445
7	4.30	-0.537

Slope = -0.133
Std. Error of Estimate = 3.4 x 10^{-2}
Variance of slope = 7.1 x 10^{-5}

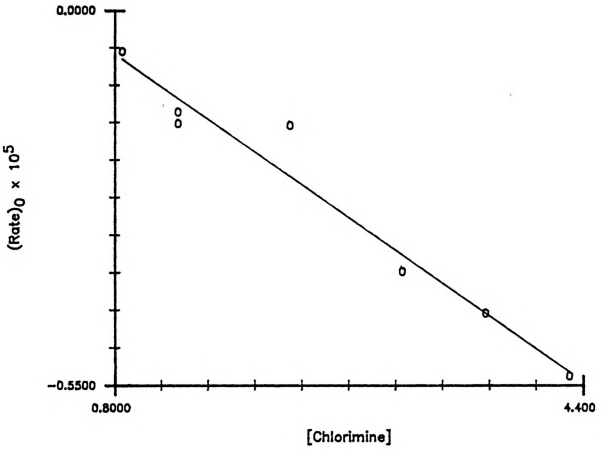

Figure 5.2 Plot of the initial reaction rate vs. the initial concentration of chlorimine. Data collected for hydrolysis of chlorimine.

TABLE 5.2
Chlorimine Hydrolysis as a Function of pH

Method*	pH	$-(Rate)_o$ A s^{-1}	k_{obs} min^{-1}	k_{obs} s^{-1}
A	9.55	1.38×10^{-6}	9.4×10^{-5}	1.6×10^{-6}
"	10.03	4.4×10^{-6}	3.0×10^{-4}	5.0×10^{-6}
"	10.53	1.08×10^{-5}	7.4×10^{-4}	1.2×10^{-5}
"	11.02	2.34×10^{-4}	1.6×10^{-3}	2.7×10^{-5}
B	7.50	1.67×10^{-6}	2.04×10^{-4}	3.40×10^{-6}
"	8.06	2.22×10^{-6}	3.57×10^{-4}	5.95×10^{-6}
"	9.76	5.00×10^{-6}	6.12×10^{-4}	1.02×10^{-5}
"	10.10	8.80×10^{-6}	9.42×10^{-4}	1.57×10^{-5}
"	10.71	2.04×10^{-5}	1.64×10^{-3}	2.73×10^{-5}
C	9.00	9.9×10^{-7}	1.1×10^{-4}	1.8×10^{-6}
"	9.25	2.21×10^{-6}	2.4×10^{-4}	4.0×10^{-6}
"	9.76	4.89×10^{-6}	5.3×10^{-4}	8.8×10^{-6}
"	10.02	6.76×10^{-6}	7.3×10^{-4}	1.2×10^{-5}
"	10.55	1.63×10^{-5}	1.8×10^{-3}	3.0×10^{-5}
"	10.99	2.05×10^{-5}	2.2×10^{-3}	3.7×10^{-5}

* Data collection method:
A indicates data from the Heath spectrophotometer.
B indicates data from the Perkin-Elmer stripchart recorder.
C indicates data from the microcomputer.

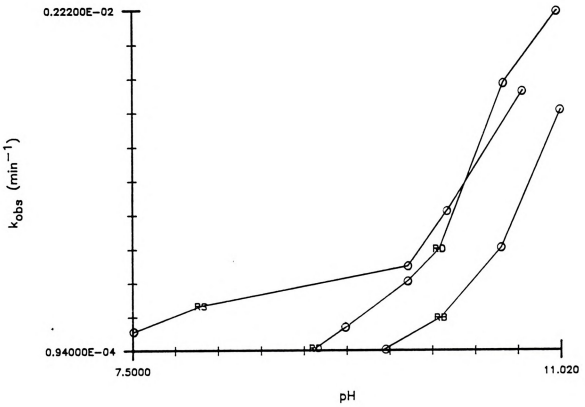

Figure 5.3 Effect of pH on the rate of hydrolysis of chlorimine. Data collected in three separate experiments. Solid lines connect values of k_{obs} obtained within any one experiment.

vs pH from these experiments. The three curves represent data collected by the three different methods. Discrepancies between the curves arise from temperature effects, as well as from the errors in determining initial rates from the data. However, all three curves show that the rate constant increases with increasing pH, indicating general base-catalyzed hydrolysis of the chlorimine.

b. The Phenol-Chlorimine Reaction

After studying the process of hydrolysis for chlorimine, experiments were performed to study the kinetics of the reaction between chlorimine and phenol. A stock solution of chlorimine was prepared by adding 1 mL of ethanol to a 100 mL volumetric flask containing 8.4 mg of chlorimine. When dissolved, 5 mL of pH 8 borate buffer were added to the flask, and the solution was diluted to volume with distilled water. This solution was refrigerated while successive 100- 2000 μL aliquots were withdrawn to prepare reagent solutions. Each aliquot was mixed with 500 μL of 0.010 M phenol, 3 mL borate buffer and enough distilled water to dilute to a total volume of 5.500 mL. Chlorimine was added as the last reagent. The mixture was shaken rapidly and placed in a cell in the Heath spectrophotometer. The cell temperature was maintained at 22.0 ± 0.2 C, and the reaction was monitored by collecting absorbance data for the appearance of indophenol. For a pseudo-first order process, a plot of the initial rate versus the initial chlorimine concentration should be linear as predicted in equation 5.1.

$$(\text{Rate})_0 = \frac{d[I]}{dt} = \frac{1}{\varepsilon b} \cdot \frac{dA}{dt} = k_1' \cdot [C] \qquad (5.1)$$

In the above equation, ε is the molar absorptivity of indophenol, b is the cell path length, I represents indophenol, and C represents chlorimine. Initial rates can be determined from the initial slope of the reaction curve. While analyzing the data to determine initial rates, an unexpected trend became apparent: the reaction rate was found to increase with time in a consistent manner throughout the collected data. This response is quite unusual since reaction rates normally decrease as the reagents are consumed. Consequently, two additional experimental runs were made to collect data over a much longer time interval. One reaction mixture was placed in a cell in the Heath spectrophotometer and absorbance data were collected for 3 hours. Another reaction mixture was placed in the Hitachi 200 spectrophotometer and data were collected for 80 minutes. The latter test was made in the double-beam instrument to ensure that drift in the lamp had not caused the apparent increase in rate. Both data sets confirm that the rate does increase with time during an initial phase of the reaction. Eventually the reaction profile assumes a more typical shape. Figure 5.4 shows the absorbance-time reaction profile for 168 minutes.

Clearly the reaction profile indicates that the reaction being studied was not simple pseudo-first order. The reaction profile shown in Figure 5.4 is similar in shape to reaction curves obtained from multi-step reactions. The reaction of chlorimine with phenol contributes, in part, to the observed reaction profile. The species responsible for the complicated mechanism was unknown. However, it is important to note that although the reaction is no longer simple pseudo-first order, the UV-VIS spectrum of the final mixture still matches that of indophenol.

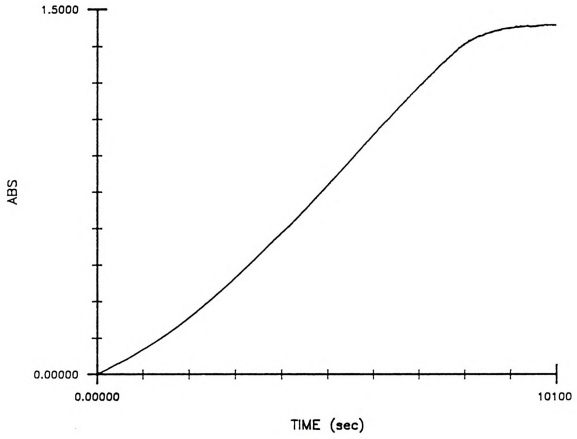

Figure 5.4 Reaction profile for the reaction between chlorimine and phenol. Absorbance data collected for 168 minutes.

Although the reaction kinetics are obviously now complicated, indophenol is still the only product that appears to form.

Svobodova and co-workers [60] determined that hydrolysis of 2,6-dichloroquinonechlorimine produces 2,6-dichloroquinoneimine. Both compounds were shown to react with phenol to produce indophenol, but the quinoneimine did so at a faster rate than the parent quinoneimine. Such a mechanism could result in a reaction curve of the same general shape as those obtained in these experiments. In solutions containing a large excess of phenol, chlorimine undergoes parallel first order reactions, given by:

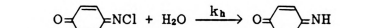

(5.2)

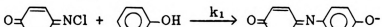

(5.3)

Equation 5.2 represents hydrolysis, which produces quinoneimine, with a rate constant given by k_h. Equation 5.3 indicates reaction with phenol to produce indophenol, with a rate constant given by k_1. In the presence of phenol, the quinoneimine formed by reaction 5.2 will also produce indophenol with a rate constant given by k_2.

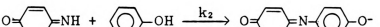

(5.4)

If $k_1 >> k_h$, hydrolysis is negligible in comparison to the rate of reaction 5.3; essentially no quinoneimine is produced. The rate of formation of indophenol would thus depend only on the concentration of chlorimine. However, if k_1 is not significantly greater than k_h, then hydrolysis will effect the rate of formation of indophenol. At time zero for the reaction the concentration of quinoneimine is zero and the initial reaction rate is proportional to the concentration of chlorimine alone. As reaction 5.3

proceeds, hydrolysis of chlorimine produces quinoneimine in a competing reaction. As quinoneimine forms, it too reacts with phenol to produce indophenol. The rate of formation of indophenol then becomes dependent on the concentration of both quinoneimine and chlorimine. The resulting rate equation could be written as:

$$\frac{d[I]}{dt} = k_1[C][PhOH] + k_2[Q][PhOH] \qquad (5.5)$$

where I represents indophenol, C represents chlorimine, Q represents quinoneimine, and PhOH is the phenol concentration. However, the observed increase in the reaction rate would occur only if $k_2 > k_1$. Values for k_h at the pH of these experiments have been determined to be in the range 1-6 x 10^{-4} min^{-1}. Pseudo-first-order values for k_1 and k_2 must be used to compare with values of k_h. Under the pseudo-first-order conditions of these experiments, the pseudo-order rate constants k_1' and k_2' are given by:

$$k_1' = k_1 \cdot [PhOH] \qquad (5.6)$$

$$k_2' = k_2 \cdot [PhOH] \qquad (5.7)$$

Corbett [59] has reported values of the rate constant for the reaction between quinoneimine and phenol. A value for k_2' at this pH and concentration of phenol is calculated to be 3.8 x 10^{-2} min^{-1}. It remains to determine the value of k_1' from the data. Since the concentration of quinoneimine is zero at the start of the reaction, the initial rate is dependent on the concentration of chlorimine alone. Under conditions of excess phenol, Equation 5.5 reduces to Equation 5.1 for time zero. Equation 5.1 indicates that k_1' can be determined from a plot of the initial rate versus initial chlorimine concentration. The data were analyzed to determine initial rates through linear regression

analysis. Table 5.3 lists the results of the analysis. A plot of initial rate vs initial concentration is shown in Figure 5.5. The resulting line indicates that equation 5.1 is valid during the initial portion of the reaction when the quinoneimine concentration is negligible. The slope of the line of Figure 5.5 provides a value for k_1'. Using $\log(\varepsilon) = 3.95$ from Patton and Crouch [17], k_1' is calculated to be 3.0×10^{-3} min^{-1}. This value is sufficiently greater than k_h that the initial portion of the reaction curve should indeed be free from hydrolysis effects. However, it is not large enough that hydrolysis of chlorimine is negligible; quinoneimine is produced in significant amounts. As quinoneimine is produced, it reacts with phenol more rapidly than does chlorimine. The effect is an increase in the rate of production of indophenol, as seen in Figure 5.4.

As is shown by the excellent linearity of Figure 5.5, it is possible to avoid the effects of hydrolysis by collecting data early in the reaction between phenol and chlorimine. The values for k_1' were determined in this manner. Equation 5.6 shows how k_1' is related to k_1 and [PhOH]. Since [PhOH] is known, k_1 is easily calculated for the reaction between chlorimine and phenol. The second order rate constant determined from this data gives $k_1 = 5.3 \times 10^{-3}$ $\underline{M}^{-1}$ s^{-1}.

A series of experiments was performed to determine the effect of pH on the rate of reaction between these reagents. A solution of phenol was prepared by dissolving 4.7484 g of the solid in a few mL of ethanol and diluting to volume with distilled water in a 100 mL volumetric flask. A series of borate buffers were prepared to cover the pH range of 7.5 to 11. Stock solutions of phenol were prepared at various pH values by adding 5 mL of the original phenol solution to 40 mL of borate buffer

TABLE 5.3
The Reaction Between Phenol and Chlorimine

Chlorimine µl	[Chlorimine]$_o$ M x 10^5	(Rate)$_o$* x 10^5
2000	21.58	10.4
1750	18.9	9.2
1500	16.2	8.4
1250	13.5	7.1
1000	10.8	6.2
800	8.63	5.4
600	6.47	4.3
400	4.32	3.4
200	2.16	2.6
100	1.08	2.0

* Initial rate values as absorbance units per second.

Slope = 0.446
Std error of estimate = 6.6×10^{-6}
Variance of slope = 9.8×10^{-4}

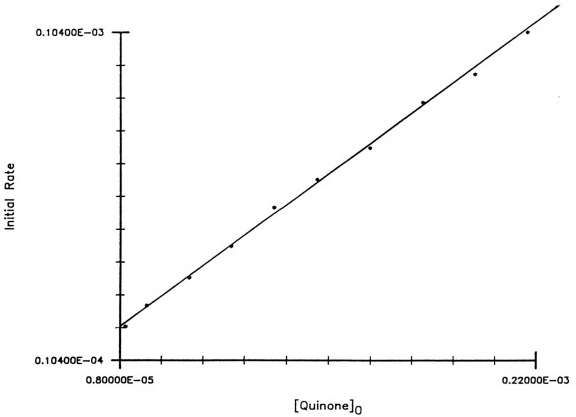

Figure 5.5 Plot of the initial reaction rate vs. the initial concentration of chlorimine for a reaction between chlorimine and phenol.

and diluting to 50 mL. One phenol stock solution was prepared for each of the borate buffer solutions. Then 3.2 mg of chlorimine were dissolved and diluted to 100 mL. This stock solution was refrigerated during the course of the experiments. To a 10 dram vial were added 5 mL of pH 7.62 borate buffer, 350 μL of phenol of the same nominal pH, and 1000 μL of the chlorimine solution. The mixture was shaken rapidly and placed in a cell in the Hitachi 200 spectrophotometer. Absorbance data were collected at 635 nm and stored by the microcomputer. This process was repeated for the solutions prepared at the various pH values. The pH of each solution was determined with a pH meter and a combination pH electrode (Orion Research). To extend the pH beyond 11, three additional solution were prepared by adjusting the pH with 1.0 M NaOH. The pH of these solutions remained constant during the reactions. As previously, initial rates were determined by linear-regression analysis of the data. Table 5.4 lists the pH values and initial rates for each of the solutions tested. Figure 5.6 shows a plot of the reaction rate as a function of pH.

As was shown by Gibbs [53,54], the reaction of quinoneimines is dependent on the concentration of phenolate ion in solution. As the pH increases, the equilibrium concentration of phenolate ion increases. Hence, for a given concentration of phenol, the rate of its reaction with chlorimine increases as the pH increases. This effect is most pronounced near pH 10 (near the pK_a of phenol) where small changes in pH result in relatively large changes in the equilibrium concentration of phenolate ion. Above a certain pH all phenol is present as phenolate ion. At this point the pH dependence of the reaction levels off; further increases in pH no longer affect the rate of the reaction. Figure 5.6

TABLE 5.4
The Phenol-chlorimine Reaction
Initial Rate as a Function of pH

pH	$(Rate)_o$ x 10^5	k_{obs} s^{-1}	[Phenolate] mM
7.62	0.037	0.0104	0.0189
8.06	0.24	0.0674	0.0516
8.53	0.52	0.146	0.147
8.99	0.29	0.082	0.386
8.99	0.32	0.090	0.386
9.46	1.64	0.461	0.895
9.91	2.5	0.702	1.59
10.14	3.7	1.04	1.93
10.33	4.9	1.38	2.17
10.53	4.7	1.32	2.36
10.92	5.7	1.60	2.59
11.51	7.1	1.99	2.73
12.04	7.8	2.19	2.76
12.57	8.1	2.28	2.78

* Initial rates as absorbance units per second.

Plot of k_{obs} vs. [phenolate] (first seven points):

Slope = 1.336

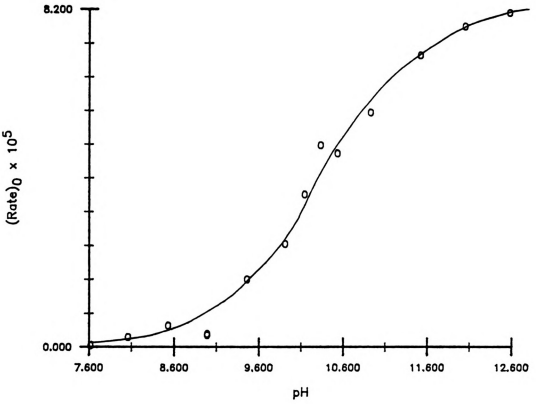

Figure 5.6 Effect of pH on the rate of reaction between chlorimine and phenol.

shows this expected trend, closely resembling a molar distribution diagram for the phenolate ion. As expected, the rate of increase in the reaction rate per unit pH is greatest in the region near the pK_a for phenol.

Attempts were made to fit a reaction model for this phenolate ion dependence to the data shown in Figure 5.6. The model fit the data well at lower pH values. However, at pH values beyond the pK_a of phenol the model levels off more rapidly than do the actual data. The data show a reaction rate which continues to increase slowly with pH beyond what the model predicts. This discrepancy can be explained due to the pH dependence of the rate of hydrolysis of chlorimine. The rate of hydrolysis of chlorimine was shown to increase with increasing pH. This results in an increase in the rate of formation of quinoneimine.

Equation 5.5 shows how the concentration of quinoneimine influences the rate of formation of indophenol. It has already been determined that quinoneimine reacts more rapidly with phenol than does chlorimine. Furthermore, the hydrolysis dependence on pH was not observed to level off as pH was increased. As the solution pH increases, more chlorimine is converted to quinoneimine within a given period. The greater the concentration of quinoneimine within a given period, the greater the rate of formation of indophenol. Thus, while the equilibrium effect of the phenolate ion on the rate levels off, the effect of increasing concentrations of quinoneimine does not. The result is that the rate of formation of indophenol continues to increase slightly with increasing pH.

C. EFFECT OF THE COUPLING REAGENT

The stability of chlorimine and the initial rate of its reaction with phenol have been examined. It was now of interest to determine the effect of SpF on this final step of the Berthelot reaction. Studies by Patton and Crouch [16,17] indicate that a molar excess of the coupling reagent AqF over NH_2Cl caused the absorption peak of the final reaction product spectrum to shift from 635 nm toward 700 nm. This section provides results of some molar ratio studies of SpF, as well as studies to examine the role of the coupling reagent SpF.

1. Experimental

Equilibrium molar ratio studies were performed by preparing stock reagents of phenol, chlorimine and SpF. Aliquots of these solutions were transferred into 10 dram vials using a micropipet (Eppendorf). The concentration of phenol was always large enough to provide pseudo-order conditions. This would match conditions found in Berthelot reaction procedures. The amounts of chlorimine and SpF were then changed such that the [SpF]/[Chlorimine] ratio would vary from about 0.1 to greater than 10. The vials were covered and the mixtures allowed to react for a minimum of 2 hours. The spectra were then recorded over the range 600-700 nm using the Hitachi 200 spectrophotometer connected to a strip-chart recorder. This entire process was repeated for solutions containing sodium hypochlorite in addition to phenol, chlorimine and SpF.

Kinetics studies were performed by preparing stock solutions of phenol containing various amounts of SpF. A stock solution of chlorimine was then prepared such that the chlorimine concentration fell within the range of concentrations of SpF. The phenol concentration was present in excess over the other two reagents. The chlorimine solution was then mixed with each of the phenol/SpF solutions in the stopped-flow instrument. Absorbance data were collected during the course of the reaction.

2. Results and Discussion

a. Equilibrium Studies

It was previously determined [16,17] that mixtures of NH_2Cl, AqF and excess phenol produced the greatest amount of indophenol when the concentration of AqF equalled that of NH_2Cl. As the concentration of AqF increased, the absorption band for the product shifted progressively toward 700 nm. This shift was accompanied by a decrease in the absorbance at λ_{max}. The resulting solutions were green rather than the characteristic blue of indophenols. It was found that the presence of hypochlorite in these reaction mixtures allowed indophenol to be produced at slightly higher AqF to NH_2Cl ratios. The product responsible for the green color was not identified. However, a similar green-colored product has been noted by Corbett [58].

Molar ratio experiments were performed to study the effect of SpF on the final product. Stock solutions of phenol, chlorimine and SpF were prepared as described in previous chapters. Various volumes of these reagents were transferred to 10 dram vials, mixed, capped and

allowed to react for at least 2 hours. Table 5.5 summarizes the experiment. Figure 5.7 shows the spectra recorded for each solution. It can be seen that as the ratio of SpF to chlorimine increases, the absorption band does indeed shift toward 700 nm. There is also a general decrease in the absorbance at λ_{max} coincident with the shift toward 700 nm. Solutions 1 and 2, with a 5 and 3.7 molar excess of SpF over chlorimine, respectively, were visibly green. These results correlate well with the results of Patton and Crouch [17].

The above procedure was repeated for mixtures of the reagents which also included hypochlorite. Table 5.6 summarizes the experiment and Figure 5.8 shows the spectra obtained for each of the solutions. The presence of hypochlorite may indeed retard the shift in the absorption band toward 700 nm. Although λ_{max} increases slowly with increasing amounts of SpF, the first significant increase in λ_{max} occurs when the SpF concentration first exceeds the hypochlorite concentration. This is easily seen in the data of Table 5.6 and Figure 5.8. Although the green product has not been identified, the molar ratio results indicate that an excess of the coupling reagent is to be avoided.

In another equilibrium study, the reactivity of SpF towards chlorimine was tested. SpF has been found to be unreactive toward all other individual Berthelot reagents and intermediates, with the exception of hypochlorite. When mixed with HOCl, the absorption band of SpF was found to shift from 440 nm to 392 nm. This corresponds to conversion of SpF to AqF and subsequent reduction of Fe(III) to Fe(II). No further reaction occurs. In the test of SpF with chlorimine, stock solutions of the two reagents were mixed in a 10 dram vial. SpF exhibited a substantial reactivity towards chlorimine; millimolar mixtures of the two

TABLE 5.5
Molar Ratio Studies

Soln.#	µL SpF	µL DDW	[SpF]x10^5	[SpF]/[C]	λ_{max}
1	2000	500	6.06	5.0	667
2	1500	1000	4.55	3.7	663
3	750	1750	2.27	1.8	654
4	500	2000	1.21	1.2	650
5	400	2100	1.01	0.98	649
6	300	2200	0.91	0.73	646
7	200	2300	0.61	0.49	642
8	100	2400	0.303	0.24	636
9	50	2450	0.167	0.13	629

The concentrations of phenol and chlorimine were constant in each solution at:

[Phenol] = 5.49×10^{-4} M

[Chlorimine] = 1.24×10^{-5} M

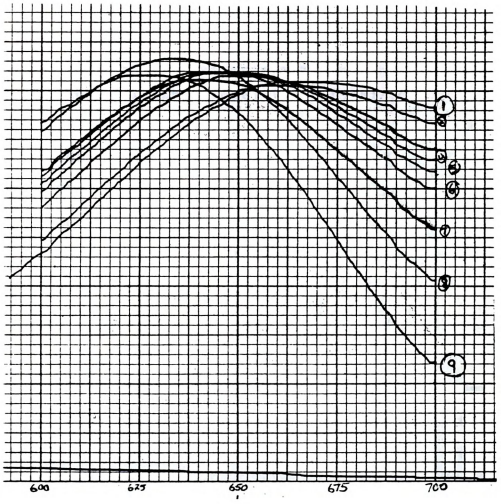

Figure 5.7 Spectra resulting from mixtures of phenol and chlorimine containing various amounts of SpF. Spectrum #1 contains the greatest concentration of SpF while #9 contains the least.

TABLE 5.6
Molar Ratio Studies
with hypochlorite present

Soln.#	µL SpF	µL DDW	[SpF]x10³	[SpF]/[C]	λ_{max}
1	3000	0	84.9	7.52	700
2	2000	1000	56.6	5.0	696
3	900	2100	25.5	2.25	665
4	800	2200	22.6	2.00	664
5	700	2300	19.8	1.75	661
6	500	2500	14.2	1.25	651
7	400	2600	11.3	1.00	650
8	300	2700	8.49	0.75	646
9	200	2800	5.66	0.50	641
10	100	2900	2.83	0.25	636
11	50	2950	1.42	0.125	630
12	10	2990	0.283	0.025	629

The concentrations of phenol, hypochlorite, and chlorimine were constant in each solution at:

[Phenol] = 5.49×10^{-4} M
[Chlorimine] = 1.24×10^{-5} M
[ClT] = 3.2×10^{-5} M

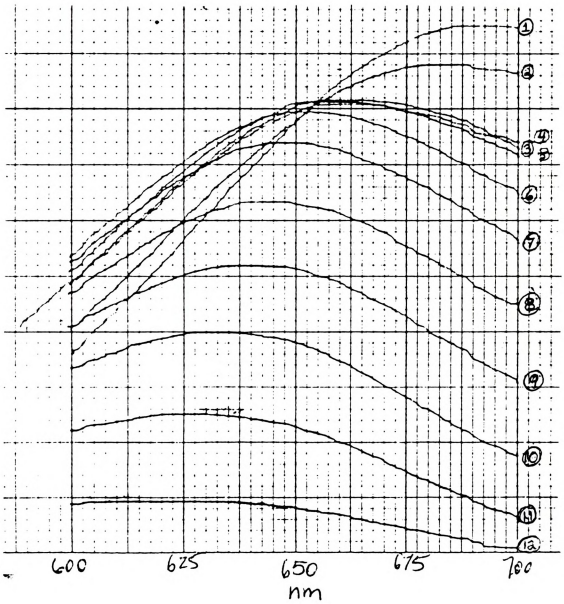

Figure 5.8 Spectra resulting from mixtures of phenol, chlorimine, HOCl and various amounts of SpF. Spectrum #1 contains the greatest concentration of SpF while #12 contains the least.

compounds were found to turn green within a matter of minutes. The spectrum of the resulting green solutions had a broad, strong absorption band with λ_{max} at 700 nm. This spectrum matches the absorption spectra of the green product obtained in the molar ratio studies above, as well as those of Patton and Crouch [17]. This same reaction would explain the formation of a green product observed by Corbett [58] in similar mixtures. The reaction responsible for the formation of the green product has thus been identified as a reaction occurring between the coupling reagent and the intermediate compound chlorimine.

b. Kinetics Studies

Results of the equilibrium studies indicate that the final step of the Berthelot reaction can be fairly complicated in the presence of SpF. It was already determined that hydrolysis of chlorimine leads to the formation of quinoneimine and that indophenol is produced by two parallel reactions. It can now be seen that chlorimine reacts with the coupling reagents to produce some unknown green product. At high concentrations of phenol and/or a molar ratio of SpF to NH_3 of roughly one or less, the reaction producing the green product is negligible; the green product is not observed under these conditions. Only at high relative concentrations of coupling reagent does the formation of green product become dominant.

No attempt was made to fully investigate this reaction. Instead, an experiment was performed to study the effect of SpF on the kinetics of the reaction between chlorimine and phenol. Using pseudo-first order conditions would simplify the data analysis. Values for k_{obs} could

be determined from a plot of the initial rate versus the initial chlorimine concentration. This value could be compared to the value for k_{obs} determined previously in the absence of SpF. This comparison would indicate the effect of the coupling reagent on the rate. Such a study must maintain a constant ratio of chlorimine to SpF. Any changes in this ratio would alter the rate data by changing the contribution due to a reaction between these two reagents. A series of chlorimine solutions were prepared over the concentration range 5.7×10^{-5} M to 3.16×10^{-6} M. A phenol-SpF solution was prepared for each chlorimine solution such that the chlorimine to SpF ratio remained constant for each reaction mixture. The phenol concentration was constant at 2.02×10^{-3} M throughout the study. The solutions were mixed in the stopped-flow instrument, and absorbance data were collected at 635 nm. It was hoped that with a high concentration of phenol, the reaction between chlorimine and SpF would have a negligible effect on the production of indophenol. Unfortunately, this was not the case for the more concentrated solutions in the series. Figure 5.9 shows a pseudo-first-order non-linear fit to the reaction data for a solution containing 1.58×10^{-5} M chlorimine. The plot of the residuals is noisy but fairly random, indicating a respectable fit. The model used for the fit was identical to the model derived for the non-linear fit in the absence of SpF. Thus SpF does not seem to alter the data even when present at four times the concentration of chlorimine. However, the model no longer fits the data for 2.37×10^{-5} M chlorimine. Reaction mixtures of the higher concentrations of chlorimine were found to develop a greenish tint; the reaction between chlorimine and SpF produces a noticeable effect for much of the data collected. The non-linear fit

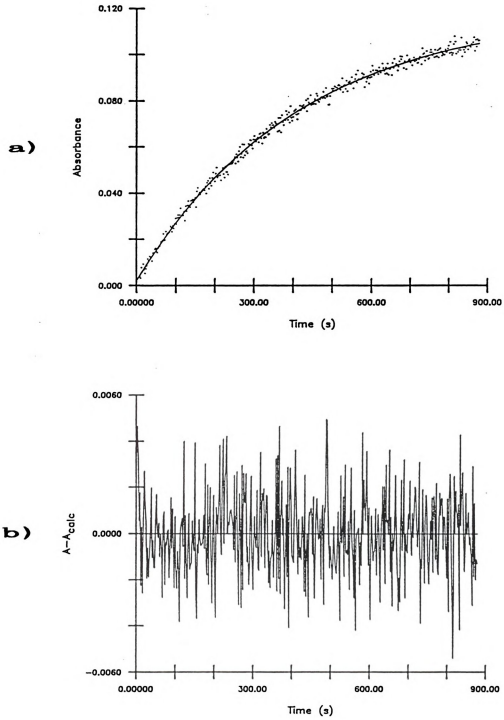

Figure 5.9 a) Non-linear pseudo-first-order fit to data collected for a reaction between phenol and chlorimine in the presence of SpF. **b)** Residuals of the non-linear fit.

value of k_{obs} was used to calculate k_1 from the solution least concentrated in SpF and chlorimine. The resulting value of 1.45×10^{-2} $\underline{M}^{-1}$ s^{-1} is roughly double the value of 5.3×10^{-3} $\underline{M}^{-1}$ s^{-1} calculated previously for k_1. However, this difference cannot be considered significant since the value for k_1 in the presence of SpF is based on the data from one solution. Furthermore, this data may well have been influenced slightly by a reaction between SpF and chlorimine, which would act to falsely increase k_{obs}. What is significant at this point is the observation that substantial quantities of SpF have very little to no effect in accelerating the reaction between chlorimine and phenol.

D. CONCLUSION

Results of this chapter were not meant to be exhaustive and complete, particularly for the kinetics of some of the interfering reactions. However, a number of important conclusions have been reached. First, hydrolysis of chlorimine was shown to be a slow, pH dependent process. Second, although hydrolysis is greatest at pH values used in typical Berthelot ammonia determinations, it does not interfere with the method since the hydrolysis product also reacts to produce indophenol. Third, the rate of the reaction between chlorimine and phenol was studied in the absence of SpF. The reaction occurs between chlorimine and the phenolate ion. The rate constant for the reaction was determined to be 5.3×10^{-3} $\underline{M}^{-1}$ s^{-1}. Fourth, the coupling reagent does not appear to act as a catalyst for the reaction between phenol and chlorimine. Finally, the green product formed during the Berthelot reaction due to the presence of excess coupling reagent has

been determined to result from a reaction between chlorimine and the pentacyanoferrate coupling reagent.

CHAPTER VI

BROMIDE INTERFERENCE STUDIES

Although the Berthelot reaction is widely used, its application for the determination of ammonia in saline solutions is restricted. Bromide ions present in saline solutions interfere severely with the Berthelot reaction. The primary interfering reaction occurs between HOCl and Br^-. The studies described in this chapter were undertaken to investigate the kinetics of this interfering reaction. A thorough understanding of the mechanism of this reaction could potentially be used to decrease (or eliminate) the interference. This would make the Berthelot reaction increasingly applicable. The literature is first reviewed to present results of prior studies concerning the reaction between HOCl and Br^-. Results obtained during the course of these studies are then presented and discussed.

A. HISTORICAL

The kinetics of the reaction between HOCl and Br^- were first reported in 1949 by Farkis, Lewin and Bloch [45]. They studied the reaction in the pH range from 10.8 to 13.4. At pH values less than 10.8, the reaction was too rapid to study using techniques available at that

time. In strongly alkaline solutions, Farkis, Lewin and Bloch were able to follow the reaction by performing titrations on samples withdrawn at periodic intervals. They were thus able to determine the total hypochlorite concentration, Cl_T, and total hypobromite concentration, Br_T, during the reaction. The concentrations of all the reaction species could be calculated from these values. Farkis and co-workers determined that the reaction occurred between undissociated HOCl and Br^-. Oxidation of Br^- to HOBr was shown to be quantitative in the presence of HOCl. The second-order rate constant for the reaction was determined to be 3.0×10^3 $\underline{M}^{-1}$ s^{-1}.

Johnson, Inman and Trofe [42] studied the reaction between HOCl and Br^- in the pH range typical of estuary waters. They used stopped-flow mixing with spectrophotometric detection to collect reaction rate data in the pH range 8.2 to 9.0. The data were analyzed by the mechanism of Farkis, Lewin and Bloch; results were stated to be consistent with this mechanism. Johnson and co-workers determined the rate constant to be 3.8×10^3 $\underline{M}^{-1}$ s^{-1} in buffered aqueous solutions. They also studied the reaction in saline solutions prepared to simulate typical estuary conditions. In such solutions the rate constant was determined to be 4.8×10^3 $\underline{M}^{-1}$ s^{-1}. The larger rate constant was postulated to be due to contributions from ion-pairing reactions.

B. KINETICS STUDIES

Farkis, Lewin and Bloch [45] analyzed their rate data by using the integrated second-order rate expression. Excellent linearity was achieved for the data plots shown. However, they were unable to study

the reaction under conditions typical of Berthelot NH_3 determinations. Johnson and co-workers [42] analyzed their data by the mechanism of Farkis, Lewin and Bloch [45] under pseudo-first-order conditions. The integrated rate expression was used to produce linear plots of the treated rate data. The slope of the resulting line was used to determine the rate constant. The 'typical' data presented by Johnson and co-workers exhibited a great deal of curvature for what should, in theory, be a straight line. This same curvature was evident in preliminary data collected on the stopped-flow instrument described in Chapter 2. This suggested that a more complex mechanism may be operative in the reaction between HOCl and Br^- under conditions less alkaline than those used by Farkis and co-workers. Since this reaction is so detrimental as an interference in the Berthelot reaction sequence, a study of the kinetics of the reaction was undertaken.

1. Reagent Preparation

a. Potassium Bromide

Potassium bromide (Fisher Scientific Company) was used as a source of bromide ion throughout these studies. Weighed amounts of the salt were dissolved in distilled water to prepare reagent concentrations ranging from 10^{-5} M to 1.00 M for stock solutions. This concentration range was sufficient to provide both second order and pseudo-first order conditions for the various studies.

b. Sodium hypochlorite

Commercially available liquid bleach was used as a stock solution for all hypochlorite solutions. The total hypochlorite concentration of the bleach was determined through iodometric titration. The standardized bleach was kept refrigerated to minimize loss of the hypochlorite. Hypochlorite solutions were prepared by diluting appropriate amounts of the standardized stock solution with distilled water.

c. Buffers

A 0.050 M sodium borate solution (Fisher Scientific Company) was prepared as a stock for all buffers. Appropriate amounts of the stock were mixed with 0.1 M HCl or 0.1 M NaOH to prepare buffers in the pH range 8 to 11.

2. Experimental

a. Rate constant determinations

Experiments to determine the rate constant were performed under a variety of conditions encompassing second order and pseudo-first order reactions. Solutions of Br^- were prepared by diluting stock solutions of KBr with buffer and distilled water. Hypochlorite solutions were prepared by diluting commercial bleach with buffer and distilled water. The reagents were allowed to reach a constant temperature in a water bath prior to reaction. The reagents were then mixed and absorbance data were collected with the stopped-flow instrument.

The following procedure was used during one experimental study. A 1.00 M KBr stock solution was prepared by dissolving the appropriate amount of KBr in distilled water in a 100 ml volumetric flask. A stock solution of hypochlorite was prepared by pipetting 15 ml of standardized bleach into a 50 ml volumetric flask and diluting with distilled water. A pH 8.80 borate buffer solution was prepared by mixing 0.05 M sodium borate with 0.1 M HCl. Then 20 ml of buffer were transferred to each of five 100 ml volumetric flasks. A micropipet was used to transfer the stock hypochlorite solution to each flask in 100 µl increments from 500-1000 µl. A Br^- solution was prepared by mixing 400 µl of stock KBr solution with 40 ml borate buffer and diluting to mark in a 200 ml volumetric flasks. Absorbance-time data for the reaction were collected with the stopped-flow instrument.

b. Equilibrium study

A hypochlorite solution was prepared by diluting 1000 µl of bleach and 50 ml borate buffer to 100 ml with distilled water. The UV spectrum of the mixture was recorded over the range 190-340 nm. The solution was then mixed in equal proportions with a solution prepared by dissolving 0.0138 g KBr in 50 ml borate buffer and 50 ml distilled water. The pH of all solutions was measured at 8.52. The spectrum of the resulting mixture was then recorded over the same UV region. NaCl was then added to the mixture in increments roughly equivalent to 25% of the Br^- concentration. UV spectra were recorded for the solution following each NaCl addition until a final concentration of 0.2 M Cl^- was achieved.

c. Diode-array study

The reaction was also monitored using the diode-array detector connected to the stopped-flow instrument. A solution of hypochlorite was prepared by diluting 250 μl bleach and 20 ml of borate buffer to 100 ml with distilled water. A Br^- solution was prepared by diluting 1 ml of 1.00 M KBr and 20 ml borate buffer to 100 ml with distilled water. The two solutions were mixed in the stopped-flow instrument. Using the diode-array detector, absorbance data were collected over the wavelength range from 200-600 nm. The data were stored in memory and new spectral scans were recorded at 10 ms intervals. A total of 99 spectral scans were recorded during the course of the reaction. The experiment was repeated for varying reagent concentrations and detector integration times.

3. Results and discussion

The reaction between HOCl and Br^- can be written as:

$$HOCl + Br^- \longrightarrow HOBr + Cl^- \qquad (6.1)$$

Farkas, Lewin and Bloch [45] determined that the reaction was overall second order. They also determined that the reaction occurred between undissociated HOCl and Br^-. Because of the rapid equilibrium between HOCl and OCl^-, the rate of the reaction depends on the total hypochlorite concentration, Cl_T, as given previously in equation 3.5. The rate expression for the reaction can thus be written as:

$$RATE = d[Cl_T]/dt = k_{Br}[HOCl][Br^-] \qquad (6.2)$$

Equation 3.7 expresses the concentration of HOCl in terms of Cl_T. After

substitution of the right side of equation 3.7 into equation 6.2, the constant terms can be collected together to give:

$$d[Cl_T]/dt = k_{Br}'\cdot[Cl_T][Br^-] \quad (6.3)$$

$$k_{Br}' = k_{Br}\cdot(1+K_a/a_H\cdot\gamma)^{-1} \quad (6.4)$$

Where K_a is the dissociation constant for HOCl, a_H is the hydrogen ion activity and γ is the mean ionic activity coefficient. Equation 6.3 can be integrated to produce the expression given in equation 3.25. This second-order expression can be used to treat the collected reaction data. For reactions occurring in the presence of excess Br^-, the $[Br^-]$ term of equation 6.3 remains constant and can be absorbed into k_{Br}'. The resulting pseudo-first-order rate equation can be expressed as in equation 3.13. This integrated rate expression can also be used to treat the reaction data. Or, as was shown in chapter 3 for pseudo-first-order conditions, a plot of the initial rate versus the initial concentration of Cl_T should yield a straight line whose slope equals k_{Br}'. All three methods have been described more fully in previous chapters. Each method of data treatment was used to analyze data collected for this interfering reaction. Each method converts the rate expression into the form for a straight line. The treated rate data are linearized, and the rate constant can be determined from the slope of the least-squares fit. None of the methods provided completely linear plots for data collected during these studies. The integrated expressions were particularly susceptible to noise in the data collected near the end of the reaction.

Table 6.1 presents results for the experiment detailed in the experimental section. These data were analyzed with the integrated second-order rate expression shown in equation 6.3. The rate constant is calculated from the slope of the 'linear' data. Curvature in the line

TABLE 6.1
Rate constant determination for the HOCl/Br^- reaction

Solution	µl bleach	$[Cl_T] \times 10^3$	slope $\times 10^2$	k_{Br}, $M^{-1}s^{-1}$
1	500	1.00	7.89	3.06×10^3
2	600	1.20	4.22	2.03×10^3
3	700	1.40	3.33	2.13×10^3
4	800	1.60	2.40	2.28×10^3
5	900	1.80	1.36	2.49×10^3
6	1000	2.00	0.0882	2.46×10^3

Data analyzed using integrated second-order rate expression. Slopes determined through linear regression analysis of the resulting line.

Average $k_{Br} = 2.40 \times 10^3$
Std. deviation = 4×10^2
Rate constant = $(2.40 \pm 0.4) \times 10^3$

from data near the end of the reaction was ignored. The calculated rate constant is (2.4 ± 0.4) x 10^3 $\underline{M}^{-1}$ s^{-1}. The rate constant value is lower than the value from previous work [42,45]. It is however typical of the values determined from analysis of data using linear algorithms.

a. Equilibrium Studies

Farkis, Lewin and Bloch [45] reported that Br^- is quantitatively oxidized to HOBr in the presence of HOCl. The suspicion arose during the present analyses that perhaps a more complex mechanism occurred in conditions much less alkaline than those used by Farkis and co-workers. Perhaps the reaction between HOCl and Br^- reached some equilibrium or involved some of the equilibrium species of the two acids. Certainly proton exchange from HOCl to the OBr^- produced during the reaction could affect the rate. Consequently, the position of equilibrium was determined for the reaction between HOCl and Br^-. The UV spectrum of a solution of HOCl was recorded from 190 to 340 nm. A second spectrum of the solution was then recorded after the addition and dissolution of a slight molar excess of KBr. The second spectrum indicated complete conversion of Cl_T to HOBr and OBr^-. Solid KCl was then added to the solution. Equation 6.1 indicates that Cl^- is produced during oxidation of Br^-. If reaction 6.1 is actually in equilibrium, the position of equilibrium will shift upon addition of KCl. This will produce a shift in the UV spectrum for the solution; the absorption bands for Br_T would decrease while those for Cl_T would increase. Increasingly larger amounts of KCl were added to the solution up to a ten-fold molar excess over the initial Br^- concentration. In no case did the UV spectrum of the solution change. The experiment was repeated for

various solution pH values, but the added KCl never had an effect on the absorption bands of the hypobromite products. This indicates that reaction 6.1 does indeed go to completion.

b. Diode-array Studies

With the rapid, multi-wavelength detection capabilities of the diode-array spectrophotometer, it is possible to follow the appearance or disappearance of several absorbing species during a reaction. It may also be possible to observe short-lived intermediate species which may otherwise have gone undetected. Such capabilities were useful for studying the reaction between HOCl and Br^-. Data collected at a single wavelength proved difficult to linearize, as seen above. This suggested that a more complex mechanism may be operative, involving, perhaps, equilibrium forms of the reactive species. In the mechanism of Farkis, Lewin and Bloch [45], HOCl is converted to HOBr through reaction with Br^-. Both acids absorb UV radiation, as do their conjugate bases. No intermediates or other species should be visible during the reaction. Because the molar absorptivity of OCl^- is much larger than that of HOCl, and because the conjugate base predominates under typical Berthelot reaction conditions, the UV spectrum of the reacting solution at time zero is essentially that of OCl^-. As the reaction proceeds, HOCl reacts with Br^- to produce HOBr. The separate acid-base equilibria shift rapidly to produce OBr^- and to convert OCl^- into HOCl. Thus the absorption band for OCl^- decreases during the reaction while the bands for HOBr and OBr^- increase. Figure 6.1 shows the absorption bands for HOCl, OCl^-, HOBr and OBr^-, all of which are present in various amounts during the reaction. Figure 6.2 shows the UV spectra collected during

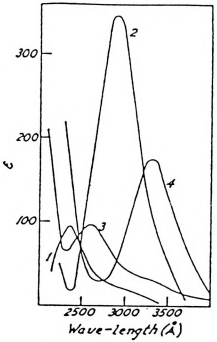

Figure 6.1 UV spectra for HOCl, OCl^-, HOBr and OBr^- (1,2,3, and 4, respectively).

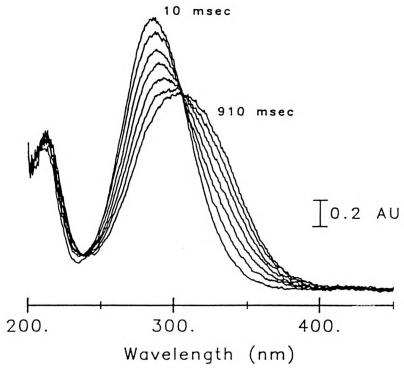

Figure 6.2 Time-dependent UV spectra for the reaction between HOCl and Br^-. Spectra recorded at periodic intervals using the diode-array spectrophotometer.

a reaction using the diode-array. The spectra are plotted at regular intervals over the course of the reaction. The absorption band for OCl^- at 292 nm is replaced by the absorption band for OBr^- at 329 nm. An isosbestic point is clearly visible at 307 nm. These data indicate that there is a direct conversion of hypochlorite to hypobromite, in support of the mechanism of Farkis, Lewin and Bloch [45].

c. Non-linear Curve-fitting

Non-linear fitting has been used successfully for the analysis of data presented in earlier chapters. The integrated rate expressions are much less sensitive to noise when written in a form suitable for non-linear fitting algorithms. The fit of the models to the data has proven to be significantly better than for linear least-squares fitting. For this reason, the non-linear fitting routine of Wentzell [44] was applied to the data which had been collected for the $HOCl/Br^-$ reaction. Data were retrieved from floppy disk storage and analyzed using the second-order model of Farkis, Lewin, and Bloch [45]. The model fit the data well with only random scatter in the residuals. Rate constants were determined from the fit parameters. The second order rate constant was found to be in the range of $(3 \pm 1) \times 10^3\ \underline{M}^{-1}\ s^{-1}$.

A detailed study of the reaction using non-linear fitting was not attempted. Results have shown that the reaction between HOCl and Br^- goes to completion. Excess amounts of Cl^- do not impede the reaction. Diode-array data indicate that the reaction does not involve intermediates or previously unaccounted-for equilibria. Solution pH does affect the rate as indicated in previous work [42,45]. This effect was accounted for in the integrated rate expressions and the reaction model

fit the data reasonably well. Results collected during these studies show that the kinetics data of Farkis and co-workers [45] does hold in the pH range typical of Berthelot NH_3 determinations. In light of this information, further investigation of the reaction was deemed redundant. Finally, as will be shown, a rate constant in the range of 10^3 $\underline{M}^{-1}$ s^{-1} makes it difficult, at best, to avoid bromide ion interferences in the normal course of the Berthelot reaction.

C. CONCLUSION

When hypochlorite is added to saline solutions containing NH_3, two parallel reactions occur:

$$HOCl + NH_3 \longrightarrow NH_2Cl + H_2O \qquad (6.5)$$

$$HOCl + Br^- \longrightarrow HOBr + Cl^- \qquad (6.6)$$

Although the latter reaction does not directly interfere with the Berthelot reaction, the HOBr formed can react with NH_3 to produce bromamines:

$$HOBr + NH_3 \longrightarrow NH_2Br + H_2O \qquad (6.7)$$

$$NH_2Br + NH_3 \longrightarrow NHBr_2 + H_2O \qquad (6.8)$$

$$NHBr_2 + NH_3 \longrightarrow NBr_3 + H_2O \qquad (6.9)$$

These reactions consume ammonia, thereby decreasing the amount of indophenol produced via the Berthelot reaction. Wajon and Morris published results from a study of the kinetics of reaction 6.7 in 1981 [62]. The rate constant for the reaction was determined to be 7.5×10^7 $\underline{M}^{-1}$ s^{-1}. This rate constant is an order of magnitude faster than the rate constant for reaction 6.5. Hence, reaction 6.7 competes effectively with the Berthelot reaction sequence. Because each mole of HOBr

produced can react with 3 moles of NH_3, significant error can arise during Berthelot NH_3 determinations. By studying the kinetics of reaction 6.6, it was hoped that reaction conditions could be chosen to reduce or eliminate the bromide ion interference.

In chapter 3, the rate constant for reaction 6.5 was determined to be 3.2 x 10^6 $\underline{M}^{-1}$ s^{-1}. The relative rates of reactions 6.5 and 6.6 can be determined from a ratio of the rate expressions

$$RATE_N = k_N \cdot [HOCl][NH_3] \tag{6.10}$$

$$RATE_{Br} = k_{Br} \cdot [HOCl][Br^-] \tag{6.11}$$

The ratio of the rate expressions reduces to

$$\frac{RATE_N}{RATE_{Br}} = \frac{k_N \cdot [NH_3]}{k_{Br} \cdot [Br^-]} \tag{6.12}$$

Substitution of equation 3.8 into equation 6.12 for $[NH_3]$ produces:

$$\frac{RATE_N}{RATE_{Br}} = \frac{k_N \cdot [N_T]}{k_{Br} \cdot [Br^-]} \cdot \frac{1}{(1 + K_b a_H / K_w \gamma)} \tag{6.13}$$

Where K_b is the base dissociation constant for NH_3, a_H is the H^+ activity, γ is the mean ionic activity coefficient, and K_w is the dissociation constant of water. The concentration of Br^- in seawater is typically near 10^{-3} $\underline{M}$, while NH_3 levels in such solutions may be below 10^6 $\underline{M}$. The relative rates of the competing reaction are calculated by substitution of the appropriate values into equation 6.13 at a fixed pH. For a solution of 10^{-3} $\underline{M}$ Br^- and 10^6 $\underline{M}$ NH_3 at pH 7, the rate of production of HOBr (equation 6.6) is roughly 230 times that of NH_2Cl (equation 6.5). Alkaline conditions will favor the production of NH_2Cl since the ammonia will be present mainly as NH_3. At pH 10, under the previous conditions, the relative rates are roughly equal; HOBr and NH_2Cl would be produced at about the same rate. However, since the

HOBr formed reacts rapidly with NH_3, a significant amount of NH_3 will still be lost to the formation of bromamines.

Given the rate constants determined for reaction 6.5 and 6.6, the concentrations of NH_3 and Br^- in typical saline solutions and the pH range in which the Berthelot reaction is performed, bromide ion interferences cannot be avoided through adjustments to the conditions used in the normal Berthelot reaction sequence. Instead, other methods must be used to eliminate bromide ion interferences. Phenol can be added as the first reagent. Reaction conditions can be chosen such that the formation of HOBr is favored upon subsequent addition of hypochlorite. HOBr reacts with phenol to form brominated phenols which do not interfere with the formation of indophenol. Furthermore, HOBr reacts with phenol at a greater rate than does HOCl [63]. This reaction can be used to reduce the Br^- concentration.

Other classical methods can also be used to remove Br^- from solution. These methods include ion-exchange beds, or precipitation of the halide with Ag^+. Although such methods may be elaborate, they must be used if no Br^- interference can be tolerated.

CHAPTER VII

FUTURE WORK

The ultimate goal of the present studies was to apply the kinetics information from the Berthelot reaction steps to develop an improved procedure for the determination of NH_3. This could best be accomplished through the use of continuous flow/flow injection techniques. The inherent flexibility of these techniques could allow reaction conditions to be optimized for each step of the Berthelot reaction sequence. As the flowing stream moves across a reaction manifold, reagents and buffers could be added where needed to enhance the desired reaction. Temperature and reaction time can easily be controlled in such a system. High throughput with excellent precision are also characteristics of continuous flow/flow injection techniques.

Before this method can be developed, two studies must first be performed. The kinetics of the reaction between chlorimine and the coupling reagent must first be determined. This information is needed to determine how best to accelerate the production of indophenol while also preventing the formation of the green product formed in chapter 5 studies. The second study involves the determination of the kinetics of the second step of the Berthelot reaction. This requires a deconvolution of data since, in the presence of coupling reagent, the second reaction step proceeds immediately into the production of indophenol. Once completed, kinetics information from these studies can be combined with the presently determined data to provide a more complete understanding

of the reaction. This knowledge should provide a base upon which an improved Berthelot reaction method can be built.

One further study could provide useful kinetics information. Conditions cannot be chosen to reduce the relative rate of reaction of HOCl with Br^-. It competes effectively with the first step of the Berthelot reaction. As mentioned in the previous chapter, HOBr formed as a result of this interfering reaction will brominate phenol present in solution [63]. This reaction does not consume NH_3 and does not interfere with the formation of indophenol. Consequently, phenol is often added first in NH_3 determinations in saline solutions. An investigation of the kinetics of this reaction could provide information beneficial to the development of an improved Berthelot method for NH_3 in saline solutions.

LIST OF REFERENCES

LIST OF REFERENCES:

1. L. Solorzano, *Limnol. Oceanogr.*, **5**, 799(1969).

2. M. Berthelot, *Repertoire de Chemie Applique*, **1**, 284 (1859).

3. P. Thomas, *Bull. Soc. Chim.*, **11**, 797 (1912).

4. J.A. Russel, *J. Biol. Chem.*, **156**, 457 (1944).

5. A.B. Crowther and R.S. Large, *Analyst*, **81**, 64 (1956).

6. B. Lubochinsky and J. Zalta, *Bull. Soc. Chem. Biol.*, **36**, 1363 (1954).

7. N.T. Bolleter, C.J. Bushman, and P.W. Tidwell, *Anal. Chem.*, **33**, 592(1961).

8. D.B. Horn and C.R. Squire, *Clin. Chim. Acta*, **14**, 185 (1966).

9. D.B. Horn and C.D. Squire, *Clin. Chim. Acta*, **17**, 99 (1967).

10. H.B. Mark, T.E. Weichselbaum, and J.C. Hagerty, *Anal. Chem.*, **41**, 848 (1969).

11. J.H. Espenson and S.G. Wolenuk, Jr., *Inorg. Chem.*, **11**, 2034 (1972).

12. V.V. Bochkarev, V.P. Lopatinskii, V.L. Ivasenko, E.M. Mogilevskaya, L.N Grebenyuk, E.V. Yurikova and I.V. Usenko, *Koord. Khim.*, **3**, 719 (1977).

13. E.B. Borghi, M.A. Blesa and P.J. Aymonino, *J. Inorg. Nucl. Chem.*, **43**, 1849(1981).

14. J.H. Swinehart and P.A. Rock, *Inorg. Chem.*, **5**, 573 (1966).

15. S. Ohkuma, *Yakugaku Zasshi*, **80**, 505(1960).

16. C.J. Patton, M.S. Thesis, Michigan State University, 1977.

17. C.J. Patton and S.R. Crouch, *Anal. Chem.*, **49**, 464 (1977).

18. P. Blanchard, C. Madec, and J. Courtot-Coupez, *Analusis*, **10**, 155(1982).

19. R.L. Searcy, N.M. Simms, J.A. Foreman, and L.M. Bergquist, *Clin. Chim. Acta*, **12**, 170(1965).

20. J.W. Harwood and D.J. Huyser, *Water Res.*, **4**, 501(1970).

21. B. Chance, *J. Franklin Inst.*, **229**, 455, 613, 737(1940).

22. S.R. Crouch, F.J. Holler, P.K. Notz, and P.M. Beckwith, *Appl. Spect. Rev.*, 13(2), 165(1977).

23. P.M. Beckwith, Ph.D. Dissertation, Michigan State University, 1972.

24. P.M. Beckwith and S.R. Crouch, *Anal. Chem.*, 44, 221(1973).

25. P.K. Notz, Ph.D. Dissertation, Michigan State University, 1977.

26. F.J. Holler, Ph.D. Dissertation, Michigan State University, 1977.

27. R.S. Gall, Ph.D. Dissertation, Michigan State University, 1978.

28. R. Balciunas, Ph.D. Dissertation, Michigan State University, 1981.

29. R.B. Putt, M.S. Thesis, Michigan State University, 1983.

30. E.H. Ratzlaff, Ph.D. Dissertation, Michigan State University, 1982.

31. B. Newcome, Ph.D. Dissertation, Michigan State University, 1983.

32. M.W. Lister and D.E. Rivington, *Can. J. Chem.*, **33**, 1572(1955).

33. J.F. Below, Jr., R.E. Connick, and C.P. Coppel, *JACS*, **80**, 2961(1958).

34. B.G. Willis, J.A. Bittikofer, H.L. Pardue, and D.W. Margerum, *Anal. Chem.*, **42**, 1340(1970).

35. J.E. Stewart, "Flow Deadtime in Stopped-Flow Measurements (Durrum Application Notes No. 4)", Durrum Instrument Corp., Sunnyvale, CA 94303.

36. D.R. Christmann, Ph.D. Dissertation, Michigan State University, 1980.

37. J.L. Dye and L.H. Feldman, *Rev. Sci. Instrum.*, **37**, 154(1966).

38. M.A. Victor, Ph.D. Dissertation, Michigan State University, 1987.

39. J.C. Merkins, *Water Waste Treatment J.*, 7, 150(1958).

40. I. Weil and J.C. Morris, *J. Am. Chem. Soc.*, **71**, 1664(1949).

41. D.W. Margerum, E.T. Gray, Jr., and R.P. Huffman, Organometals and Organometalloids, F.E. Brinkman and J.M. Bellama, eds., ACS Symposium Series 82, American Chemical Society, Washington, 1978, pp. 278-291.

42. J.D. Johnson, G.W. Inman, Jr. and T.W. Trofe, "Cooling Water Chlorination: The Kinetics of Chlorine, Bromine, and Ammonia in Sea Water", NUREG/CR-1522, U.S. Nuclear Regulatory Commission, Washington, 1982.

43. J.W. Moore and R.G. Pearson, "Kinetics and Mechanism", 3rd Edition, John Wiley & Sons, New York, 1981.

44. P.D. Wentzel, Ph.D. Dissertation, Michigan State University, 1987.

45. L. Farkas, M. Lewin, and R. Bloch, *J. Am. Chem. Soc.*, 71, 1988(1949).

46. R.G. Bates and G.D. Pinching, *J. Am. Chem. Soc.*, **72**, 1393(1950).

47. G. Emschwiller, *Compt. Rend. Acad Sci. (Paris)*, **238**, 341(1954).

48. E.J. Baran and A. Muller, *Z. Anorg. Allgm. Chem.*, **368**, 144(1969).

49. K.A. Hofmann, *Ann. Chem.*, **312**, 1(1900).

50. J. Kleinberg, M. Techotyky, and L.F. Audrieth, *Anal. Chem.*, 26, 1388(1954).

51. Robiquet, *Ann. Chem.*, **15**, 289(1835).

52. A. Hirsch, *Ber. Chem. Ges.*, **12**, 1903(1880).

53. H.D. Gibbs, *J. Biol. Chem.*, **72**, 649(1927).

54. H.D. Gibbs, *J. Phys. Chem.*, **31**, 1053(1927).

55. L.M. Kulberg and L.D. Borzova, *Ukrain Khim. Zhur.*, **22**, 100(1956).

56. L.K.J. Tong, *J. Phys. Chem.*, **58**, 1090(1954).

57. J.F. Corbett, *J. Chem. Soc. (B)*, 207(1969).

58. IBID, 213(1969).

59. IBID, 1502(1970).

60. D. Svobodova, P. Krenek, M. Fraenkl, and J. Gasparic, *Mikrochimica Acta*, 251(1977).

61. D. Svobodova, P. Krenek, M. Fraenkl, and J. Gasparic, *Mikrochimica Acta*, 197(1978).

62. J.E. Wajon and J.C. Morris, *Inorg. Chem.*, 21, 4258(1982).